

# Benzoylformate Decarboxylase from *Pseudomonas putida* as Stable Catalyst for the Synthesis of Chiral 2-Hydroxy Ketones\*\*

Hans Iding,<sup>[a]</sup> Thomas Dünwald,<sup>[b]</sup> Lasse Greiner,<sup>[c]</sup> Andreas Liese,<sup>\*,[c]</sup> Michael Müller,<sup>\*,[b]</sup> Petra Siegert,<sup>[a]</sup> Joachim Grötzinger,<sup>[d]</sup> Ayhan S. Demir,<sup>[b]</sup> and Martina Pohl<sup>\*,[a]</sup>

**Abstract:** The thiamin diphosphate- and Mg<sup>2+</sup>-dependent enzyme benzoylformate decarboxylase (BFD) from *Pseudomonas putida* was characterized with respect to its suitability to catalyze the formation of chiral 2-hydroxy ketones in a benzoin-condensation type reaction. Carboligation constitutes a side reaction of BFD, whereas the predominant physiological task of the enzyme is the non-oxidative decarboxylation of benzoylformate. For this purpose the enzyme was obtained in sufficient purity from *Pseudomonas putida* cells in a one-step purification using anion-exchange chromatography. To facilitate the access to pure BFD for kinetical studies, stability investigations, and syn-

thetical applications, the coding gene was cloned into a vector allowing the expression of a hexahistidine fusion protein. The recombinant enzyme shows distinct activity maxima for the decarboxylation and the carboligation beside a pronounced stability in a broad pH and temperature range. The enzyme accepts a wide range of donor aldehyde substrates which are ligated to acetaldehyde as an acceptor in mostly high optical purities. The enantioselectivity

**Keywords:** decarboxylation • enzyme catalysis • enzyme membrane reactors • stereoselective synthesis • thiamin diphosphate

of the carboligation was found to be a function of the reaction temperature, the substitution pattern of the donor aldehyde and, most significantly, of the concentration of the donor aldehyde substrate. Our data are consistent with a mechanistical model based on the X-ray crystallographic data of BFD. Furthermore we present a simple way to increase the enantiomeric excess of (*S*)-2-hydroxy-1-phenyl-propanone from 90% to 95% by skillful choice of the reaction parameters. Enzymatic synthesis with BFD are performed best in a continuously operated enzyme membrane reactor. Thus, we have established a new enzyme tool comprising a vast applicability for stereoselective synthesis.

[a] Dr. M. Pohl, Dr. H. Iding, P. Siegert (enzymology)  
Institut für Enzymtechnologie  
Heinrich-Heine Universität Düsseldorf im  
Forschungszentrum Jülich, 52426 Jülich (Germany)  
Fax: (+49)2461-612490  
E-mail: ma.pohl@fz-juelich.de

[b] Dr. M. Müller, Dr. T. Dünwald, Prof. Dr. A. S. Demir<sup>[+]</sup> (bioorganic chemistry)  
Institut für Biotechnologie 2  
Forschungszentrum Jülich GmbH, 52425 Jülich (Germany)  
Fax: (+49)2461-613870  
E-mail: mi.mueller@fz-juelich.de

[c] Dr. A. Liese, L. Greiner (reaction engineering)  
Institut für Biotechnologie 2  
Forschungszentrum Jülich GmbH, 52425 Jülich (Germany)  
Fax: (+49)2461-613870  
E-mail: a.liese@fz-juelich.de

[d] Dr. J. Grötzinger (molecular modeling)  
Institut für Biochemie der RWTH Aachen  
Pauwelsstr. 1, 52074 Aachen (Germany)

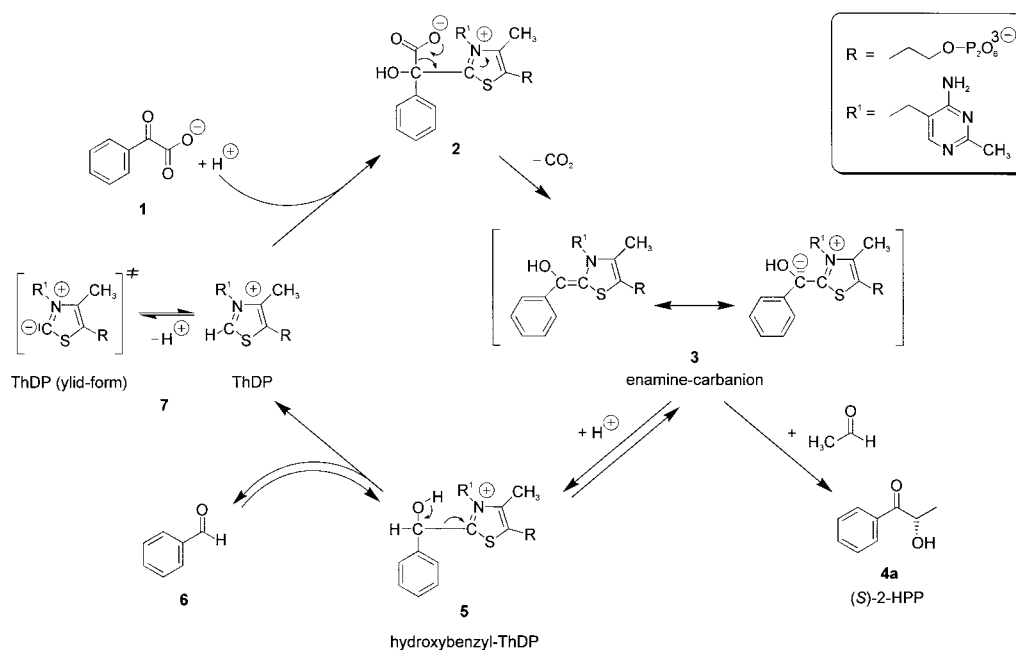
[+] Department of Chemistry  
Middle East Technical University, 06531 Ankara (Turkey)

[\*\*] The abbreviations used are: BFD: benzoylformate decarboxylase, CSTR: continuous stirred tank reactor, EDTA: ethylenediaminetetraacetic acid, His: hexahistidine, HLADH: horse liver alcohol dehydrogenase, 2-HPP: 2-hydroxy-1-phenyl-propanone (2-hydroxy propiophenone), MOM: methoxymethyl, NTA: nitrilotriacetic acid, PAGE: polyacrylamide gel electrophoresis, PDC: pyruvate decarboxylase, ThDP: thiamin diphosphate, wt: wild type.

## Introduction

Benzoylformate decarboxylases (BFD, E.C. 4.1.1.7)\*\* have been found in bacteria such as *Pseudomonas putida*, *Acinetobacter calcoaceticus*, and *Pseudomonas aeruginosa*.<sup>[1–3]</sup> The enzyme is involved in the degradation of aromatic compounds of the mandelate catabolism. Only BFD from *P. putida* has been examined in detail so far. The coding gene was cloned<sup>[4]</sup> and the crystal structure was published recently.<sup>[5]</sup> The spatial arrangement of the four subunits in the crystal is similar to pyruvate oxidase from *Lactobacillus plantarum*<sup>[6]</sup> and to pyruvate decarboxylase (PDC) from *Zymomonas mobilis*.<sup>[7]</sup> The main enzymatic reaction catalyzed by BFD is the non-oxidative decarboxylation of benzoylformate to benzaldehyde. There are many evidences that the reaction mechanism (Scheme 1) is similar to that of pyruvate decarboxylases.<sup>[8, 9]</sup>

Initial studies found the substrate range of the decarboxylation reaction to be restricted to aromatic 2-keto acids.<sup>[8, 9]</sup> We focused our interest on the ability of the enzyme to catalyze the enantioselective C–C-bond formation, which constitutes a side reaction of hitherto unknown physiological function. Besides thiamin diphosphate (ThDP) dependent<sup>[10, 11]</sup> decarboxylases,<sup>[12, 13]</sup> only a few synthetically useful



Scheme 1. Reaction mechanism of the BFD-mediated decarboxylation of benzoylformate and the carboligation of the activated benzaldehyde with acetaldehyde yielding (*S*)-2-HPP. A common intermediate of both reaction pathways is the enamine-carbanion species **3** consisting of benzaldehyde bound to ThDP (“Umpolung” of benzaldehyde). The release of benzaldehyde from hydroxybenzyl-ThDP is a reversible step. Thus, carboligation does not require a previous decarboxylation step. BFD mediates carboligation, if the ThDP-bound “active aldehyde” (acyl donor) is ligated to a further aldehyde (here: acetaldehyde) acting as an acyl acceptor.

enzymes are able to catalyze C–C-bond formation.<sup>[14]</sup> Among these are oxynitrilases, aldolases, and transketolases.<sup>[15]</sup>

ThDP-dependent decarboxylases catalyze a benzoin-condensation type reaction resulting in chiral 2-hydroxy ketones. The mechanistic aspects of ThDP-mediated reactions have been discussed by Kluger<sup>[16]</sup> and Kern and co-workers.<sup>[17]</sup> The enzymatically catalyzed reaction should be a versatile stereoselective alternative to the classical benzoin condensation.<sup>[18]</sup> Some chemical methods have been evolved using non-chiral<sup>[19]</sup> and chiral<sup>[20]</sup> thiazolium and triazolium salts for catalysis of this C–C-bond forming reaction. 2-Hydroxy ketones in general are important structural subunits in many biologically active natural products and are also important synthons for stereoselective syntheses.<sup>[21]</sup> Several methods have been developed for the preparation of such optically active compounds. Among them are the stereoselective oxidation of titanium enolates with dimethyldioxirane,<sup>[22]</sup> of silyl enol ethers with chiral salen complexes,<sup>[23]</sup> or fructose derived dioxirane,<sup>[24]</sup> and the stereoselective dihydroxylation of enolates with *N*-sulfonyloxaziridines.<sup>[25]</sup> As an alternative to chemical methods enantiomerically pure 2-hydroxy ketones are prepared enzymatically by reduction of the diketone<sup>[26]</sup> or kinetic resolution of the racemate of either 2-peroxy,<sup>[27]</sup> 2-hydroxy,<sup>[28]</sup> or 2-acetoxy ketones.<sup>[29]</sup> A well-known industrial example for a chemoenzymatic reaction pathway comprising the formation of the 2-hydroxy ketone (*R*)-phenylacetylcarbinol ((*R*)-PAC) as chiral precursor in the synthesis of L-ephedrine is mediated by yeast or isolated PDC.<sup>[12, 30]</sup>

Although the synthetic potential of PDC has been characterized in detail,<sup>[13]</sup> only little is known on the substrate and product range of BFD. Wilcocks and co-workers<sup>[31, 32]</sup>

described the formation of (*S*)-2-hydroxy-1-phenyl-propanone ((*S*)-2-HPP) and the corresponding derivatives, when BFD-catalyzed decarboxylation of benzoylformate or benzoylformate derivatives is performed in the presence of acetaldehyde. However, the finding that (*S*)-2-HPP was formed with an optical purity of only 91–92% in batch experiments<sup>[31]</sup> suggests that BFD from *P. putida* is a less useful catalyst for enantioselective syntheses than PDC.

The aim of this study was to characterize the synthetic potential of BFD from *P. putida*. In detail we focused on: i) the characterization of the substrate and product range of the enzyme, ii) factors influencing the optical purity of the 2-hydroxy ketones formed, iii) investigations of the enzyme stability and kinetic parameters, and iv) the evaluation of a continuous process for the formation of chiral 2-hydroxy ketones.

We describe a simple method to obtain the biocatalyst from *P. putida* or from a recombinant *Escherichia coli* strain in high amounts, free of interfering side activities. Further, we present an effective method to increase the optical purity of the desired 2-hydroxy ketones by a skillful choice of the reaction temperature and the substrate concentration. Our results show that BFD is a powerful catalyst for the enantioselective formation of various aromatic and even aliphatic (*S*)-2-hydroxy ketones using aldehydes instead of 2-keto acids as sole substrates.

## Results

**Preliminary remarks:** Since the main catalytic activity of BFD, the decarboxylation of benzoylformate, is by a factor of

40 higher than the carboligase reaction, and easy to determine in a continuous photometric assay, we used the decarboxylation of benzoylformate as a measure for the catalytic activity during purification and stability investigations.

**Fermentation and purification of BFD from *P. putida*:** *P. putida* strain ATCC 12633 was grown in a medium containing D-*L*-mandelic acid as the only carbon source. A 200 L fermentation yielded about 150 000 U BFD with a specific decarboxylase activity of 2.2 U mg<sup>-1</sup> in the crude cell extract (Table 1). The purification procedures reported so far required a joint action of an ammonium sulfate precipitation and various chromatographic steps,<sup>[1, 4, 31, 33]</sup> resulting in BFD preparations with specific decarboxylase activities in the range of 17 to 193 U mg<sup>-1</sup>, depending on the addition of cofactors to the purification buffers. We omitted the ammonium sulfate precipitation step from the purification protocol and reduced the procedure to an anion-exchange chromatography and a subsequent desalting step. This purification resulted in a ten-fold increase of the specific activity (Table 1) and yielded the enzyme sufficiently pure for the application in biotransformations, since interfering enzyme activities (e.g. oxidoreductases) were efficiently removed. Pure enzyme with a specific decarboxylase activity of 230 U mg<sup>-1</sup> was obtained by affinity chromatography on an affi-blue column.<sup>[33]</sup> However, this method is limited to small-scale purifications.

**Cloning, expression, and purification of BFD-His:** The availability of the cloned BFD-gene<sup>[4]</sup> offered an easier way to purify BFD for enzymological and protein chemical investigations. The protein sequence revised upon analysis of the crystallographic data<sup>[5]</sup> is depicted in Figure 1. Using the vector pBFD/trc<sup>[4]</sup> as a template, the gene was elongated by six codons for histidine at the 3'-end. Expression of the modified gene encoding BFD with a C-terminal hexahistidine tail (BFD-His) in *E. coli* SG13009 yielded about 10–15% BFD-His among the total soluble cell protein. The enzyme was purified to homogeneity in one chromatographic step on a Ni-NTA-agarose resin. The resulting specific decarboxylase activity of 320 U mg<sup>-1</sup> is significantly higher than that of wt-BFD obtained by affinity chromatography on affi-blue agarose (230 U mg<sup>-1</sup>) (Table 1). Both protein fractions appeared to be homogenous in a silver-stained PAGE (data not shown). A possible interpretation of the discrepancy might be partial protein inactivation during the dye-affinity chromatography.

## Studies on the decarboxylation reaction and the enzyme stability

*i) pH Dependence of the decarboxylation reaction:* The ThDP-mediated decarboxylation of 2-keto acids includes various protonation and deprotonation steps (Scheme 1).<sup>[8, 9]</sup> Thus, the pH dependence of the reaction was investigated under initial rate conditions using the direct decarboxylase assay. The results are summarized in Figure 2. BFD exhibits a relative decarboxylase activity of 80–100% in the range of pH 5.5–7.0, with a distinct maximum at pH 6.2. The lower activity at pH < 5.5 is likely due to the low stability of the enzyme in the acidic pH range. The deactivation kinetic of BFD-His is almost linear with 0.3% min<sup>-1</sup> at pH 5.5, whereas at pH 3 deactivation is exponential. However, BFD is stable at pH 8 and is slowly deactivated at pH 10 (0.1% min<sup>-1</sup>).

*ii) Temperature dependence of the decarboxylation reaction:* Increase of the temperature from 30 °C to 68 °C increased the decarboxylase activity by a factor of 4.5 (Figure 3). From these data the activation energy of the decarboxylase reaction has been calculated to 38 kJ mol<sup>-1</sup> using the Arrhenius equation. The enzyme is stable up to a temperature of 60 °C for 2 h, but is inactivated rapidly at 80 °C (half-life period: 15–20 min).

## Kinetic constants and substrate range of the decarboxylation reaction:

BFD shows a hyperbolic velocity versus substrate concentration (*v*/*S*) plot with a *K<sub>M</sub>* value of 0.7 mM for benzoylformate (data not shown). *V<sub>max</sub>* varied between 230 U mg<sup>-1</sup> for the wt-enzyme purified by dye-affinity chromatography and 320 U mg<sup>-1</sup> for BFD-His (Table 1). The substrate range of the decarboxylation reaction using purified enzyme is shown in Table 2. Although BFD is highly specific for benzoylformate, it exhibits low activities with some aliphatic 2-keto acids. Among these, best results were obtained with 2-oxo-hexanoate. Since decarboxylation and carboligation take place at the same active site and have a common transition state (Scheme 1), this result indicates that aliphatic aldehydes may bind as acyl donors to the active center.

**Stability of the cofactor binding:** In ThDP- and Mg<sup>2+</sup>-dependent decarboxylases cofactors are bound non-covalently which makes addition of the cofactors to the reaction buffer necessary.<sup>[12]</sup> Thus, we studied the stability of the cofactor binding in BFD. ThDP-free BFD is easily obtained by elution of BFD-His from the Ni-NTA-matrix during purification

Table 1. Purification of wt-BFD from 1360 g *P. Putida* cells (200 L culture volume) and BFD-His from 98 g *E. coli* SG13009 cells carrying the pBFD-His plasmid (20 L culture volume).<sup>[a]</sup>

Purification step	Total activity/U	Specific activity/U mg <sup>-1</sup>	Purification factor	Yield per step/%
crude extract ( <i>P. putida</i> )	150 000	2.2	1	100
anion-exchange chromatography/desalting	142 500	22	10	70
dye-affinity chromatography <sup>[a]</sup>	7.5	230	105	15
crude extract ( <i>E. coli</i> )	175 000	60	1	100
Ni-NTA chromatography/desalting (gel filtration)	140 000	320	5	80

[a] 2.3 mg of BFD (50 U) purified by anion-exchange chromatography were subjected to dye-affinity chromatography.

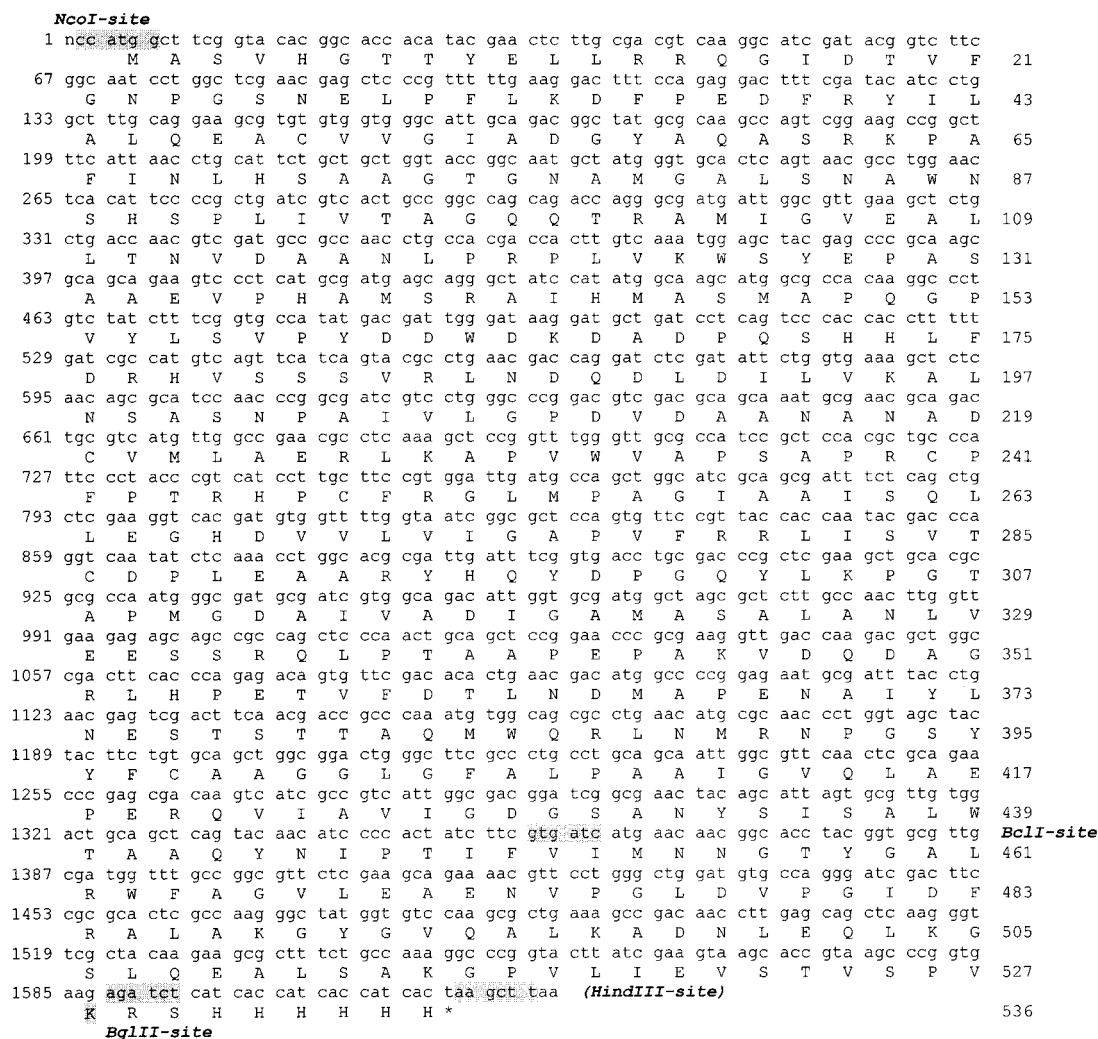


Figure 1. Protein and DNA sequence of BFD–His from *P. putida* revised upon structural analysis.<sup>[5]</sup> The restriction sites used for cloning are indicated (grey). The wt-sequence is terminated with K528. BFD–His is elongated by eight amino acid residues at the C-terminus.

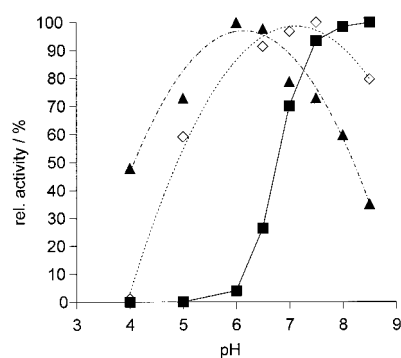


Figure 2. Determination of pH optima: (▲) Decarboxylation of benzoylformate using the direct decarboxylase assay, (◇) carbonylation yielding (S)-2-HPP using benzoylformate and acetaldehyde as substrates, and (■) carbonylation yielding (S)-2-HPP using benzaldehyde and acetaldehyde as substrates.

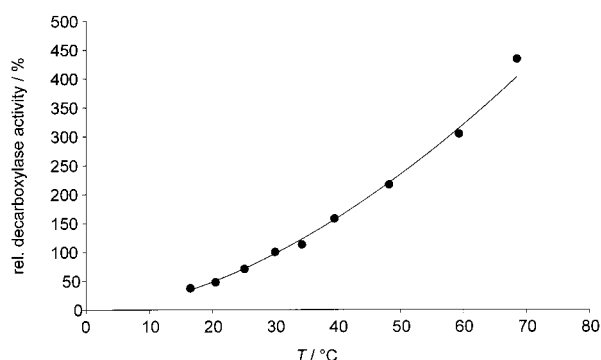


Figure 3. Temperature dependence of the BFD-mediated decarboxylation of benzoylformate. Data were obtained using the direct decarboxylase assay. An activation energy ( $E_a$ ) of 38 kJ mol<sup>-1</sup> was calculated according to Arrhenius for the decarboxylation of benzoylformate using the following equation:  $\log V_{\max} = \log A - E_a/(2.303 RT)$ .

using ThDP-free buffer, whereas Mg<sup>2+</sup> is bound tightly to the enzyme. Even incubation in the presence of 10 mM EDTA for 16 h at 40 °C resulted in only slight removal (20%) of bound Mg<sup>2+</sup>. Demonstrating the significant stabilizing effect of ThDP and Mg<sup>2+</sup>, the inactivation of BFD in the absence of

cofactors in comparison to a cofactor containing enzyme preparation is shown in Table 3 by means of the half-life of the enzyme activity. Additionally, the inactivating effects of benzaldehyde and acetaldehyde on the enzyme are investigated.

Table 2. Relative decarboxylase activity of BFD–His towards various 2-keto acids. The activity was obtained using the coupled decarboxylase assay.

2-Keto acid	Relative activity/%
2-Oxo-2-phenylacetate (benzoylformate)	100
2-Oxo-3-phenyl-propanoate (phenylpyruvate)	0
3-Cyclohexyl-2-oxo-pentanoate	0.07
4,4-Dimethyl-2-oxo-pentanoate	0.05
4-Methyl-2-oxo-pentanoate	0.43
3-Methyl-2-oxo-pentanoate	0.88
2-Oxo-octanoate	0.66
2-Oxo-hexanoate	1.93
2-Oxo-pentanoate	0.98
2-Oxo-butanoate	0.32
2-Oxo-propanoate (pyruvate)	0.03

Table 3. Inactivation of BFD in 50 mM phosphate buffer (pH 7) in the absence of cofactors ThDP and Mg<sup>2+</sup> in comparison to cofactor containing buffer (0.5 mM ThDP, 0.5 mM Mg<sup>2+</sup>). The influence of benzaldehyde (BA) and acetaldehyde (AA) is also investigated.

Cofactors	Temperature/°C	BA /mmolL <sup>-1</sup>	AA/mmolL <sup>-1</sup>	Half-life /d
+	4	–	–	139 ± 60
+	20	–	–	36 ± 7
+	20	–	100	1.8 ± 0.1
+	20	–	200	1.5 ± 0.1
+	20	25	–	5.3 ± 0.7
–	20	–	–	3 ± 0.4

Reconstitution of ThDP-free BFD–His was studied by incubating the apo-enzyme with increasing amounts of ThDP. The regained decarboxylase activity was determined after 24 h (data not shown). Half-maximal activity is obtained with <1 μM ThDP. A similar K<sub>0.5</sub> value (0.7 μM) has been reported for PDC from *Z. mobilis*.<sup>[34]</sup>

**Substrate and product range of the carboligation:** The potential of BFD to catalyze C–C-bond formation was first reported by Wilcocks and co-workers.<sup>[31]</sup> They observed the formation of (*S*)-2-HPP if benzoylformate was decarboxylated in the presence of acetaldehyde. A detailed analysis of 2-hydroxy ketones available from benzoylformate, benzaldehyde, and acetaldehyde as substrates resulted in the formation of three different products, (*S*)-2-HPP, (*R*)-benzoin, and (*S*)-acetoin. Among these, the heterologous carbinol (*S*)-2-HPP is formed with a specific carboligase activity of about 7 U mg<sup>-1</sup> BFD (1 U carboligase activity equals the amount of enzyme which catalyzes the formation of 1 μmol of the respective 2-hydroxy ketone per min at 25 °C, pH 7.0), whereas the specific activity of the enzyme with respect to the formation of the homologous products (*R*)-benzoin (0.25 U mg<sup>-1</sup>) and (*S*)-acetoin (<0.01 U mg<sup>-1</sup>) is significantly lower. Nevertheless, all carbinols, except acetoin, are obtained with high enantiomeric excess (Table 4). These results demonstrate that BFD has a potential for application in stereoselective synthesis to form enantiomerically pure and high enantiomerically enriched 2-hydroxy ketones. One advantage is the possibility to use aldehydes without a previous decarboxylation step instead of the corresponding high-priced α-keto acids. Thus, further

Table 4. Substrate and product range of BFD. Reactions were studied in batch syntheses and stopped after 20 h. If not stated otherwise the absolute configuration of the 2-hydroxy ketone is (*S*). All reactions<sup>[a]</sup> used acetaldehyde as an acyl acceptor.

Acyl donor	2-Hydroxy ketone	No.	Con- version/%	ee/%
		<b>4a</b>	99	92
		<b>5</b> <sup>[a]</sup>	0.4 <sup>[b]</sup>	> 99 ( <i>R</i> )
		<b>6</b>	n.d.	13
		<b>4b</b> X = Cl, Br, OMe <b>4c</b> Me <b>4d</b> X = F <b>4e</b> Cl <b>4f</b> Br <b>4g</b> Me <b>4h</b> OMe <b>4i</b> OEt <b>4j</b> OiPr <b>4k</b> OMOM <b>4l</b> OAc <b>4m</b> OH <b>4n</b> CN	0 4 91	– n.d. 89
		<b>4o</b> X = F <b>4p</b> Cl <b>4q</b> Br <b>4r</b> Me <b>4s</b> OMe <b>4t</b> OH <b>4u</b> CN	100 94 68 99 94 91 62 88 80 62 95	87 94 96 97 96 97 > 99 > 99 > 99 92 92
		<b>4v</b> X, Y = F <b>4w</b> OMe	69 85 42 65 23 11 89	87 82 83 88 92 86 74
		<b>7a</b> X = NH <b>7b</b> O <b>7c</b> S	0 56 50	– 45 83
		<b>8</b>	65	87
		<b>9</b>	21	61
		<b>10</b>	50	94

[a] Except for the synthesis of benzoin. [b] Conditions for batch synthesis, see Experimental Section.

studies were undertaken to determine the characterization of the substrate range, the steric and electronic influences of substituents both on the benzene moiety of the donor

aldehyde as well as on acetaldehyde, acting as acyl acceptor. As depicted in Table 4, BFD is able to bind a broad range of different aromatic, heteroaromatic, and even cyclic aliphatic and conjugated olefinic aldehydes to ThDP (**3**) prior to ligation to acetaldehyde. Best results with respect to optical purity of the resulting 2-hydroxy ketones were obtained with *meta*-substituted benzaldehydes. Using these substrates, the enantiomeric excess (*ee*) increased to more than 99%. With the corresponding *para*-substituted substrates a significant decrease of both the conversion rate and, in most cases, the enantioselectivity was observed. Thus, the optical purity of the ligation product depends on structural variation of the donor aldehyde. Our studies demonstrate that the sterical demand of the substituent plays a decisive role in both conversion rate and *ee*. The *ee* increases with bulky groups attached to the benzene ring (cf. the series of 3-alkoxy substituents, Table 4), but simultaneously the conversion rate decreases. Furthermore, for the first time we could demonstrate the BFD-mediated stereoselective coupling of two aliphatic substrates, cyclohexane carbaldehyde, and acetaldehyde. The significant lower conversion rate of cyclohexane carbaldehyde compared with cyclohexene and aromatic carbaldehydes to the corresponding 2-hydroxy ketones might be a consequence of missing stabilizing interactions in the active site of the enzyme. Aromatic edge-to-face interactions and, perhaps, a more favorable conformation and better delocalisation of the negative charge in state **3** (see Scheme 1, see Discussion) favor the plain aromatic substrates in the cavity of the active site in comparison to aliphatic ones. In contrast, *ortho*-substituted benzaldehyde derivatives, except 2-fluorobenzaldehyde, are only poorly accepted, probably due to sterical hinderance.

In a second approach we focused on the influences of electronic properties of the substrate affecting the biotransformation. Applying benzaldehyde substituted with groups exhibiting strong electron withdrawing effect, we found a slight decrease of conversion rate and *ee* (cf. F, CN). Moreover, amino- and nitrosubstituted substrates as well as pentafluorobenzaldehyde are not accepted by BFD (data not shown).

Apart from acetaldehyde, which is the most efficient acyl acceptor in the series tested, BFD shows low activity with benzaldehyde forming optically pure (*R*)-benzoin (Table 4). However, the synthesis of acetoin proves that acetaldehyde may also bind to the active center (Scheme 1), which is consistent with weak decarboxylase activity towards pyruvate (Table 2). Nevertheless, in the presence of benzaldehyde no ligation was observed with propionaldehyde, 2-chloro-acetaldehyde, glycolaldehyde, acrolein or propinal.

### Studies on the formation of (*S*)-2-HPP (**4a**)

*i*) *Kinetic constants of the carboligation reaction*: Results of kinetic investigations of the (*S*)-2-HPP formation using aldehydes as substrates are shown in Figure 4. The enzyme activity as a function of the benzaldehyde concentration is in accord with a Michaelis–Menten type kinetic, restricted by the solubility of benzaldehyde in aqueous solution ( $\approx 50$  mM). For acetaldehyde the initial rates were fitted by the Michaelis–Menten equation up to the maximum velocity at a

concentration of about 750 mM. Higher acetaldehyde concentrations lead to a decrease of the initial reaction rate which might be interpreted in terms of substrate inhibition or, more likely, rapid enzyme inactivation. The kinetic parameters of the following double substrate Michaelis–Menten model were fitted to the data measured under initial reaction condition by means of non-linear regression.

$$v = \frac{V_{\max} \cdot [\text{benzaldehyde}] \cdot [\text{acetaldehyde}]}{(K_{M, \text{benzaldehyde}} + [\text{benzaldehyde}]) \cdot (K_{M, \text{acetaldehyde}} + [\text{acetaldehyde}])} \quad (1)$$

The kinetic parameters calculated from Equation (1) are  $K_M$  values of 310 mM ( $\pm 80$  mM) for acetaldehyde and 77 mM ( $\pm 19$  mM) for benzaldehyde.  $V_{\max}$  was calculated to 48 U mg<sup>-1</sup> ( $\pm 10$  U mg<sup>-1</sup>). The model represents the experimental data with a reasonable correlation higher than 96% (Figure 4). However, in this case  $V_{\max}$  is only of theoretical value using aqueous buffer for biotransformation because of the limited solubility of benzaldehyde ( $K_M$  is greater than the maximal solubility of about 50 mM).

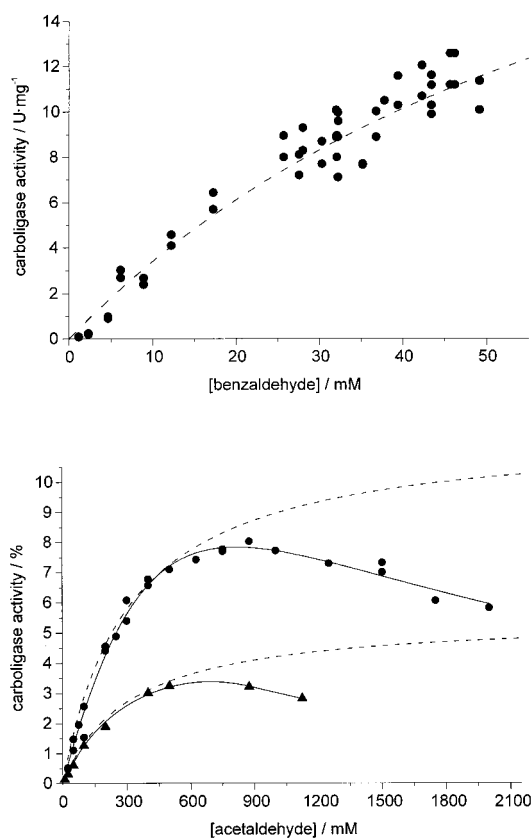


Figure 4. Determination of kinetic constants of BFD–His for the carboligation of benzaldehyde and acetaldehyde to (*S*)-2-HPP:  $v/[\text{benzaldehyde}]$ -plot obtained in the presence of 500 mM acetaldehyde (top);  $v/[\text{acetaldehyde}]$ -plot obtained in the presence of 10 mM ( $\blacktriangle$ ) and 25 mM ( $\bullet$ ) benzaldehyde, respectively (bottom). Data were fitted according to Michaelis–Menten as double substrate kinetics (dashed line). Best correlation with the experimental data was obtained by including terms for substrate-excess inhibition into the kinetic model (straight line).

*ii*) *Influence of temperature and pH value on the enzymatic carboligation*: As demonstrated for the decarboxylation reaction (Figure 3), carboligation strongly depends on the temperature (Figure 5). The carboligation activity is en-

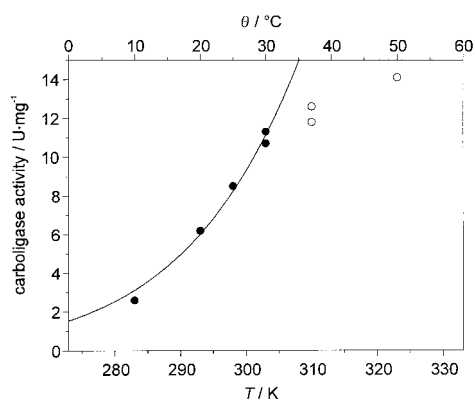


Figure 5. Influence of the reaction temperature on the carboligase activity of BFD–His. Benzaldehyde (25 mM) and acetaldehyde (500 mM) were incubated with 6.4 U BFD in standard buffer at the given temperatures. Reactions were stopped at equivalent conversion points. The plot is assimilated to Arrhenius up to 30 °C (●). The appreciation at higher temperatures (○) is minor as implicated by the Arrhenius plot.

hanced by a factor of about 2 by raising the temperature from 25 °C to 40–50 °C. However, the *ee* of the resulting (*S*)-2-HPP depends on the temperature in an inverse manner, as demonstrated in Figure 6. It has to be mentioned that the lower optical purity obtained at higher reaction temperatures is a function of the enzyme selectivity rather than of the stability of (*S*)-2-HPP. The pH optimum of the carboligation reaction is different for benzaldehyde or benzoylformate as primary substrates (Figure 2). In the first case, the formation of the carbanion-enamine **3** (Scheme 1) is a result of the nucleophilic attack of the ThDP-ylide on the carbonyl C-atom of benzaldehyde. The pH optimum for the carboligation of benzaldehyde and acetaldehyde to yield (*S*)-2-HPP was determined to pH  $\geq 8$ . Using benzoylformate and acetaldehyde as substrates the pH optimum for the carboligation is shifted to pH 7.0, since a previous decarboxylation step with a pH optimum at pH 6.2 is required.

iii) *Influences on the enantioselectivity of (S)-2-HPP (4a) formation*: The enantioselectivity of the carboligation to (*S*)-2-HPP was found to be a function of temperature, and benzaldehyde concentration. The results are shown in Figure 6. Highest *ee* values ( $>94\%$ ) were obtained using a low

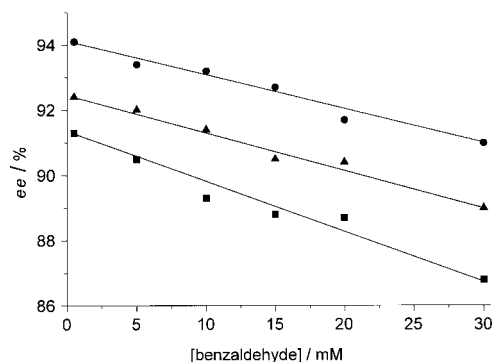


Figure 6. Influences on the enantiomeric excess of (*S*)-2-HPP: Influences on the *ee* with respect to the benzaldehyde concentration and reaction temperature were studied in batch experiments with 500 mM acetaldehyde and the depicted benzaldehyde concentrations at 4 °C (●), 20 °C (▲), and 30 °C (■).

concentration of the donor substrate benzaldehyde ( $<1$  mM) and performing the enzymatic coupling at low temperatures (4 °C). Similar high *ee* values ( $\approx 95\%$ ) for (*S*)-2-HPP can also be obtained using benzoylformate as primary substrate, but at low temperatures ( $\leq 5$  °C) and with low decarboxylation conversion rates, which coincides with a low benzaldehyde concentration (initial rate conditions, data not shown). Another fact favors a low concentration of benzaldehyde to obtain best results in the formation of (*S*)-2-HPP: In the presence of high concentration of benzaldehyde a competitive reaction yielding (*R*)-benzoin becomes more important (see Discussion).

**Continuous synthesis of (*S*)-2-HPP (4a) in the enzyme membrane reactor**: To establish a low benzaldehyde concentration during the reaction, which is needed to reach a high *ee* (see above), a continuously operated stirred tank reactor (CSTR) equipped with an ultrafiltration membrane (enzyme membrane reactor) was used.<sup>[35]</sup> BFD is retained by the ultrafiltration membrane, whereas the substrates, products and cofactors can pass the membrane. The enzyme membrane reactor works under product efflux conditions, meaning that the concentrations in each volume element are the same as at the outlet of the reactor. If steady state conditions are reached, the concentrations are independent of time and place. This enables the application of a high benzaldehyde concentration (10 mM) at the inlet, which in case of 90% conversion results in an actual concentration of 1 mM in the reactor. The conversion is controlled by enzyme concentration and residence time. The enzyme membrane reactor was operated continuously over a period of 180 h (Figure 7, data

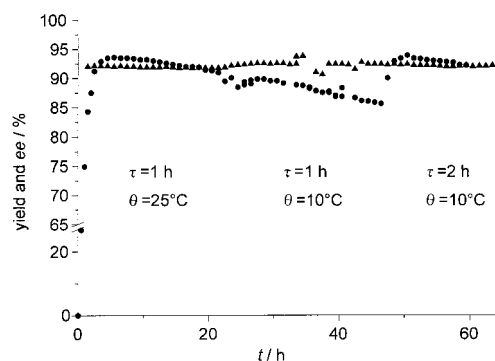


Figure 7. Progression of the conversion (●) of benzaldehyde and acetaldehyde to (*S*)-2-HPP (**4a**) using a continuously operated stirred tank reactor. Additionally, the progression of *ee* (▲) and the residence times  $\tau$ , which are adjusted to the conversion rate, are shown.

shown 0–70 h). (*S*)-2-HPP was produced with an enantiomeric excess of 92.5% and a space–time yield of 34.2 g L<sup>-1</sup> d<sup>-1</sup> (220 mmol L<sup>-1</sup> d<sup>-1</sup>). By changing the reaction temperature of the CSTR from 25 °C to 10 °C the influence of the temperature on the *ee* could be verified.

## Discussion

BFD [E.C. 4.1.1.7] is a stable biocatalyst which is available in large scale quantities by fermentation of either *P. putida* or a

recombinant *E. coli* strain carrying the BFD-gene. BFD is the most active ThDP-dependent 2-keto acid decarboxylase known so far which catalyzes both the decarboxylation (main reaction) and the carboligation (side reaction) with high specific activities. As an example 1 mg BFD-His catalyzes the decarboxylation of 320  $\mu\text{mol}$  benzoylformate per minute or the formation of 7  $\mu\text{mol}$  (*S*)-2-HPP by the coupling of benzaldehyde and acetaldehyde under standard conditions, respectively.

In earlier investigations the substrate range of the decarboxylation reaction was found to be limited to *meta*- and *para*-substituted benzoylformate derivatives.<sup>[1, 8, 9]</sup> In the present study, we found low decarboxylase activity even with some aliphatic 2-keto acids (Table 2). However, among these BFD exhibited maximal activity of only 2% (related to benzoylformate) with 2-oxo hexanoate. These results suggest that the binding of aromatic substrates is preferred through stabilization by specific supramolecular interactions in the active site of the enzyme (e.g. optimal steric fit of planar aromatic substrates, edge-to-face interactions of the phenyl ring of the substrate with Phe397 and Phe464). Scheme 2 shows the amino acid residues surrounding the active site as deduced from the crystal structure of BFD.<sup>[5]</sup> In order to visualize preferential or unfavorable contacts during the transition state of the catalytic reaction, benzaldehyde was bound to the C2-atom of the thiazolium ring by means of computer modeling<sup>[36]</sup> based on X-ray crystallographic data.<sup>[5]</sup> The spatial arrangement of the phenyl ring and the thiazole ring in the carbanion-enamine **3**, which constitutes a common transition state of both the decarboxylation and the carboli-

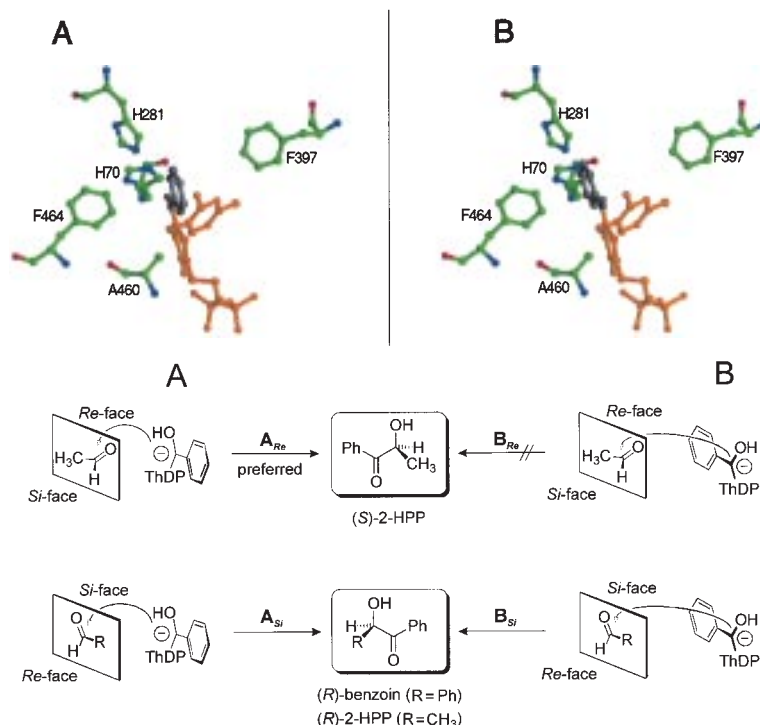
gation (Scheme 1), is probably coplanar. Under these conditions delocalisation of the negative charge is possible. In addition, the phenyl ring of benzaldehyde as shown in conformation **A** (Scheme 2) is probably arranged between the two phenyl rings of Phe464 and Phe397, which are directed approximately perpendicular, a stabilizing edge-to-face conformation frequently found in proteins.<sup>[37]</sup> Due to the partial single bond character of the C–C bond in the transition state, **3** may exist in many conformations differing in the binding angle between phenyl ring and thiazolium ring and in their orientation relative to the surrounding amino acid side chains. The conformations **A** and **B** given in Scheme 2 represent two extremes, both exhibiting a coplanar arrangement of phenyl ring and thiazolium ring. However, conformation **B** is unfavored since the edge-to-face interactions of the phenyl moiety of the substrate with Phe464 and Phe397, which are probably stabilizing conformation **A**, are missing and, in addition, the phenyl ring gets in close proximity to His70 which is discussed to be mechanistically important.<sup>[5]</sup>

Based on this central thesis of two different conformations of state **3**, which are in a kinetically controlled equilibrium (see below), we developed a model which explains the substrate range and the different effects on the enantioselectivity of the carboligation reaction which we have observed.

Assuming this model, there are four theoretically possible transition states during carboligation, which result from *Re*- and *Si*-attack on an acceptor aldehyde (e.g. acetaldehyde or benzaldehyde, Scheme 2), respectively. This model implies that catalytic processes occur only in the cavity restricted by Ala460, Phe464, His70, the protein backbone, and ThDP. In

principle, four more possible transition states are conceivable assuming that **A** and **B** attack the acceptor aldehyde from the contrary site (direction of Phe397). However, this alternative seems to be implausible because of the shielding effect of the ThDP-pyrimidine moiety on the nucleophilic center in **3** due to the V-conformation of the cofactor.

Depending on the conformation of **3** and the structure of the acceptor aldehyde, different favorable orientations relative to each other can be deduced. Based on this model we will first explain the different enantioselectivities depending on the acceptor aldehyde, resulting in (*S*)-2-hydroxy ketones with acetaldehyde and (*R*)-benzoin with benzaldehyde as an acceptor. As demonstrated in Scheme 2, in principle, two different possibilities for the formation of (*S*)- and (*R*)-products assuming *Re*- and *Si*-attack of **A**



Scheme 2. Two possible orientations of the donor substrate-ThDP complex at the active site of BFD are shown: Computer modeled complex based on X-ray crystallographic data (top) and schematic representation of the *Re*- and *Si*-attack of carbanion-enamines **A** and **B** (bottom). Preferred orientation **A<sub>Re</sub>** leads to (*S*)-2-HPP, whereas the unfavored orientations **A<sub>Si</sub>** and **B<sub>Si</sub>** are proposed to result in the formation of the minor enantiomer (*R*)-2-HPP and the by-product (*R*)-benzoin. (abbreviations: A: alanine, H: histidine, F: phenylalanine).



and **B** on the acceptor aldehyde are possible. However, the structural environment of the active site limits these possibilities to one favored orientation for acetaldehyde ( $\mathbf{A}_{Re}$ ) and two less preferred for benzaldehyde ( $\mathbf{A}_{Si}$ ,  $\mathbf{B}_{Si}$ ).

Both transition states, *Re*-attack of **A** and *Si*-attack of **B** on the acceptor aldehyde, have the relative orientation of the functional groups of acceptor and **3** in common. In both cases the carbonyl group of the acceptor approaches the phenyl moiety of **3**, whereas the methyl or phenyl group approaches the former carbonyl-*O*-atom of the ThDP-bound aldehyde. *Re*-Attack of **A** on the acceptor aldehyde implies that the methyl group of acetaldehyde is located in the small cavity defined by Phe464, His70, the protein backbone, and ThDP. Since this cavity is only accessible for acetaldehyde an absolute configuration of (*S*) of the corresponding 2-hydroxy ketones is explainable. On the other hand, acceptor aldehydes with a major steric demand, like benzaldehyde, do not fit into this cavity and are thus being attacked by **3** from the *Si*-face. Thus, all 2-hydroxy ketones obtained with larger acceptor aldehydes than acetaldehyde shall have an absolute configuration of (*R*), which is in accord with our experimental results (Table 4).

Furthermore, we proved (*R*)-benzoin to be formed enantiomerically pure, whereas the *ee* of (*S*)-2-HPP was found to be a function of the reaction temperature and, surprisingly, of the benzaldehyde concentration (Figure 6). As we have already pointed out, benzaldehyde has only one possibility to fit into the cavity of the active site and the carbologation must be a consequence of a *Si*-attack of **B** or, alternatively, *Si*-attack of **A**, which implies an approximation of the phenyl moiety of the donor and acceptor aldehyde. Both cases result in the formation of (*R*)-benzoin which explains the high optical purity (*ee* > 99%). However,  $\mathbf{A}_{Si}$  seems to be disadvantageous in the case of the formation of (*R*)-benzoin because of an unfavored arrangement to each other of the acceptor- and donor-carbonyl moieties. *Re*-Attack of **A** or **B** seems to be improbable since the cavity restricted by Phe464, His70, the protein backbone, and ThDP is appropriate only for small molecules like acetaldehyde.

The situation is different for 2-HPP, since acetaldehyde can be attacked from the *Re*- and *Si*-face by **A** and, additionally, from the *Si*-face by **B**. *Si*-Attack of **A** on acetaldehyde demands that the acceptor aldehyde is orientated with the carbonyl group towards the cavity restricted by Phe464, His70, the protein backbone, and ThDP. This orientation ( $\mathbf{A}_{Si}$ ) is vigorously unfavored in comparison to  $\mathbf{A}_{Re}$  due to a repulsive arrangement of the participating groups of the acceptor and the ThDP-bound donor aldehyde. Assuming a kinetically controlled equilibrium between both **A** and **B**, the unusual concentration dependency of *ee* can be explained. Higher concentration of the donor aldehyde results in an enrichment of species **B** and thus the *Si*-attack ( $\mathbf{B}_{Si}$ ) on acetaldehyde yielding (*R*)-2-HPP gains a major relevance. These two aspects give the rationale for the incomplete and concentration dependent chiral induction (highest *ee* obtained: 95%) of BFD in the case of the formation of (*S*)-2-HPP (**4a**). The formation of (*R*)-benzoin, which depends also on the benzaldehyde concentration, can be explained in the same way.

*Re*-Attack of **B** cannot occur, since the described cavity is shielded by the phenyl moiety of **3** and, thus, the methyl group of the acceptor aldehyde is restricted from fitting into it. However, highest enantioselectivities were obtained at low temperature (4 °C) with small benzaldehyde concentration (< 1 mM) (Figure 6), a substrate concentration significantly lower than  $K_M$  ( $77 \pm 19$  mM) (Figure 4). Accordingly, an increase of the kinetic energy by elevation of the reaction temperature would influence the rate-determining step between orientations **A** and **B** and thus increase the formation of (*R*)-2-HPP via both the  $\mathbf{A}_{Si}$ - or  $\mathbf{B}_{Si}$ -attack of acetaldehyde. The fact that the catalytic activity with respect to the formation of (*R*)-benzoin is significantly lower than for (*S*)-2-HPP can be taken as a proof for the lower concentration of **B** compared with **A**.

The last observation to be explained is the preference of aromatic donor aldehydes and the influence of their structure on the enantioselectivity of the carbologation. If we assume that orientation **A** is the most likely one, the preference for aromatic substrates is reasonable since they allow delocalisation of  $\pi$ -electrons and they can profit from the stabilizing edge-to-face interactions with Phe464 and Phe397. Also, their plain structure is sterically preferable for an optimal fit into the cavity between the two phenyl rings of the phenylalanine residues.

Donor aldehyde substrates larger than benzaldehyde should increase the energy barrier between **A** and **B**. Furthermore, the *Si*-attack ( $\mathbf{A}_{Si}$ ) described above of such a bulkier species **3** (e.g. ThDP-bound **4j**, Table 4) in conformation **A** becomes less plausible, since this orientation of the acceptor (acetaldehyde) is sterically hindered by the substituents attached to the benzene moiety. The high enantioselectivity obtained with various *meta*-substituted benzaldehyde derivatives (Table 4) may be taken as a confirmation of this hypothesis. In contrast, *para*-substituted donor substrates did not show such a distinct effect on the *ee* of the desired substituted (*S*)-2-HPP derivatives. This result seems to be due to the more stretched geometry of *para*-substituted aromatic molecules resulting in a less effective shielding of the  $\mathbf{A}_{Si}$ -attack. On the other hand *ortho*-substituted donor aldehyde substrates showed an extreme effect. Only *ortho*-fluorobenzaldehyde can react to the desired product **4c** with high yields, but substrates with bulkier groups attached to the *ortho*-position are not accepted by BFD. This observation is in accordance with an approximation of the *ortho*-substituent to the activated carbonyl moiety of **3** (cf. Scheme 2) and, thus, a strong steric shielding protects those substrates from reaction.

The presented model is fully consistent with our achieved experimental observations. It further implies that only substrates which generate carbanion-enamines **3** with a high kinetic barrier between orientation **A** and **B** can be transformed enantioselectively to the corresponding 2-hydroxy ketones in common batch synthesis (e.g. bulky substituents in *meta*-position). Less enantioselective transformations given in Table 4 are likely to be a consequence of the described mechanism. The diminished optical purity of these products obtained seems to reflect an intrinsic property of BFD.

However, our studies in batch and continuous reaction systems have demonstrated that the performance of batch

experiments is not the most useful way to obtain enantiomerically pure 2-hydroxy ketones with this enzyme. During batch synthesis, the concentrations of substrates and products change continuously,<sup>[38]</sup> which significantly influences the optical purity of the product and the amount of (*R*)-benzoin formed by a competing reaction. Additionally, BFD is inactivated by high concentrations of benzaldehyde (Table 3). We demonstrated that these problems can be circumvented by using a continuously operated stirred tank reactor (CSTR) with a high influx concentration of benzaldehyde maintaining a low concentration in the reactor itself, while working under product efflux conditions. These conditions are a prerequisite to obtain a high enantiomeric excess for (*S*)-2-HPP (**4a**) and a high space-time yield.

## Conclusion

We have established a new enzyme tool for enantioselective C–C-bond formation comprising an expandable applicability for stereoselective synthesis. BFD-mediated carbonylation of two aldehydes represents an efficient method leading to chiral 2-hydroxy ketones with a high synthetic potential. Our results open the way for the application of BFD in organic synthesis by offering highly enantiomerically enriched starting materials.

## Experimental Section

**General methods:** All reagents used were analytical grade. Cyclohexene-1-carboxaldehyde,<sup>[39]</sup> 3-ethoxybenzaldehyde,<sup>[40]</sup> 3-isopropoxybenzaldehyde,<sup>[40]</sup> 3-acetoxybenzaldehyde,<sup>[40]</sup> and 3-(methoxymethoxy)-benzaldehyde<sup>[41]</sup> were synthesized according to published procedures. If not specified, the enzymatical experiments have been performed in a buffer consisting of potassium phosphate (50 mM, pH 6.0) containing MgSO<sub>4</sub> (2.5 mM), and ThDP (0.1 mM). If not otherwise stated BFD activity is related to the decarboxylation of benzoylformate. 1 U is defined as the amount of enzyme that decarboxylates 1 μmol benzoylformate per minute at 30 °C in potassium phosphate buffer at pH 6.0. Cell disintegration was performed by using a disintegrator S (Euler, Germany). Thin-layer chromatography was carried out on aluminium sheets precoated with silica gel 60 F<sub>254</sub> (Merck). Chromatograms were inspected by UV-light (λ = 254 nm). Preparative isolation of 2-hydroxy ketones was carried out by column chromatography on silica gel 60 (mesh size 40–63 μm). Analysis of 2-hydroxy ketones was performed using HPLC (HP series 1100, Hewlett Packard), fitted with a diode array detector, and equipped with a RP-C18 column (Hypersil, 250 × 3 mm, C&S, Germany; acetonitrile/water 40:60, flow 0.3 mL min<sup>-1</sup>, 25 °C) or a chiral phase column Chiralcel OB (Daicel Ltd., 250 × 4 mm, equipped with a precolumn, 80 × 4 mm; *n*-heptane/isopropanol 9:1, flow 0.75 mL min<sup>-1</sup>, 25 °C). Gas chromatography (GC) was carried out on a Chrompack CP9002 using a column packed with Cyclodex β-1/P (Hewlett Packard, 50 m × 320 μm, T<sub>injector</sub> = 200 °C, T<sub>column</sub> = 150 °C, isotherm). Optical rotation was measured on a polarimeter 241 (Perkin–Elmer). NMR spectra were recorded on a AMX300 (Bruker Physik AG, Germany), the chiral shift reagent Eu(tfc)<sub>3</sub> (Fluka) was used for determination of *ee*. GC-MS spectra were determined on a HP 6890 series GC-system fitted with a HP 5973 mass selective detector (Hewlett Packard; column HP-5MS, 30 m × 250 μm; T<sub>GC</sub>(injector) = 250 °C, T<sub>MS</sub>(ion source) = 200 °C, time program (oven): T<sub>0min</sub> = 60 °C, T<sub>3min</sub> = 60 °C, T<sub>14min</sub> = 280 °C (heating rate 20 °C min<sup>-1</sup>), T<sub>19min</sub> = 280 °C).

**Fermentation and storage of *P. putida*:** *P. putida* ATCC 12633 was stored in an aqueous nutrient medium (Difco) containing meat extract (3%) and peptone (5%) at –80 °C. The strain was grown in the same medium in shaking flasks (500 mL) and stored on nutrient medium agar plates. One

agar colony was loop inoculated into a tube filled with mandelate medium (5 mL),<sup>[42]</sup> consisting of:

91.2 vol% potassium phosphate buffer (50 mM, pH 7.0), containing ammonium sulfate (7.5 mM), 1 vol% nutrient element solution, containing ZnSO<sub>4</sub>·7H<sub>2</sub>O (4.22 g L<sup>-1</sup>), CaCl<sub>2</sub>·2H<sub>2</sub>O (67 g L<sup>-1</sup>), FeSO<sub>4</sub>·7H<sub>2</sub>O (4.48 g L<sup>-1</sup>), MnSO<sub>4</sub>·H<sub>2</sub>O (4 g L<sup>-1</sup>), Na<sub>2</sub>MoO<sub>4</sub>·2H<sub>2</sub>O (9.25 g L<sup>-1</sup>), CuSO<sub>4</sub>·5H<sub>2</sub>O (39.2 g L<sup>-1</sup>), Co(NO<sub>3</sub>)<sub>2</sub>·6H<sub>2</sub>O (2.5 mg L<sup>-1</sup>), citric acid (10 g L<sup>-1</sup>), Titriplex III (250 g L<sup>-1</sup>), and H<sub>3</sub>BO<sub>3</sub> (2 g L<sup>-1</sup>), 2 vol% *D*-/*L*-mandelic acid/NaOH solution (1 M, pH 7.0), 5.8 vol% MgSO<sub>4</sub> (0.4 M), in citric acid (0.1 g L<sup>-1</sup>).

An overnight culture was used to inoculate a 1 L-shaking culture in a 5 L-Erlenmeyer flask, containing the same medium. After further 12 h at 30 °C a 30 L-fermentor, containing mandelate medium (20 L), was inoculated with this culture (1 L). As fermentation conditions we used 500 rpm, 30 °C, inlet air 0.34 volumes/fermentor volume/min (VVM). After 6 h with a continuous supply of mandelic acid (10 mM) the optical density (OD, 600 nm) reached a level of 3–4. The whole fermentor content was used to inoculate a 200 L-fermentor. Fermentation was carried out as described above except for inlet air (1.5 VVM). The fermentation progress was controlled using the *p*O<sub>2</sub> and the redox potential as a measure for the mandelate concentration, which was continuously supplied. The 200 L-fed-batch fermentation was carried out for 5.5 h until an OD = 4 was reached. Subsequently, cells were harvested by a chamber separator and stored at –20 °C.

**Cell disintegration and purification of BFD:** A cell suspension (40%) was prepared in potassium phosphate buffer (50 mM, pH 6.0), containing MgSO<sub>4</sub> (2.5 mM) and ThDP (0.5 mM). Cells were disrupted mechanically with glass beads (φ = 0.3 mm). After centrifugation (10 000 rpm, 4 °C) the supernatant was collected. BFD was isolated from the crude extract by anion exchange column chromatography (Q-Sepharose FF (Pharmacia), φ = 5 cm, V = 180 mL, flow 2.5 mL min<sup>-1</sup>). The column was equilibrated with potassium phosphate buffer (50 mM, pH 6.0), containing ThDP (0.15 mM), MgSO<sub>4</sub> (2.5 mM), and NaCl (0.2 M). After the elution of non-bound proteins was completed, a linear gradient of NaCl (0.2 M to 0.4 M) in the same buffer was started. BFD was eluted in the range of 275–315 mM NaCl. Desalting by gel-filtration on Sephadex G 25 (Pharmacia) yielded BFD with a specific activity of 22 U mg<sup>-1</sup>.

Dye-affinity chromatography was performed on Cibacron blue agarose (Biorad). The column (45 mL, φ = 1.6 cm) was equilibrated with potassium phosphate buffer (10 mM, pH 6.0), containing MgSO<sub>4</sub> (0.2 mM). Enzyme-bound ThDP was partially removed from the enzyme by a further desalting step. Elution of BFD (230 U mg<sup>-1</sup>) was achieved with ThDP (5 mM) in the same buffer.

**Cloning of BFD–His:** The original plasmid pBFD/trc<sup>41</sup> was used as a template for the polymerase chain reaction (PCR) to introduce a new *Bg*III site into the BFD-gene, thereby deleting the stop codon (Figure 1). The following primers were used:

5'-GGG CCA TGG CTT CGG TAC ACG G-3' (includes the *Nco*I site)

5'-CCC AGA TCT CTT CAC CGG GCT TAC-3' (includes the *Bg*III site)

The PCR-fragment was ligated into pMOSBlue-T-vector (Amersham) and the resulting vector was restricted with *Nco*I and *Bg*III (Boehringer). The gene coding for BFD was ligated to the equally restricted vector pQE60 (Qiagen). Since the expression of recombinant BFD was not possible in this vector, it was restricted with *Bcl*II and *Hind*III and the fragment containing the 3'-end of the BFD-gene including six histidine codons was ligated into the equally restricted pBFD/trc vector. The resulting vector pBFD–his was transformed into *E. coli* SG13009/prep4 (Qiagen).

**Expression and purification of BFD–His:** Expression and purification of BFD–His was performed as described for PDC<sup>43</sup> using potassium phosphate buffer (50 mM, pH 7.0) for Ni–NTA-chromatography and potassium phosphate buffer (50 mM, pH 6.0), containing ThDP (0.15 mM) and MgSO<sub>4</sub> (2.5 mM) as elution buffer for the subsequent gel chromatography. Lyophilized BFD–His stored at –20 °C was stable for several months.

**Direct decarboxylase assay:** The assay was performed by addition of BFD solution (50 μL, 0.25 U) to the substrate buffer (950 μL) consisting of potassium phosphate (150 mM, pH 6.0), MgSO<sub>4</sub> (2.5 mM), ThDP (0.5 mM), and benzoylformate (25 mM), and previously equilibrated at 30 °C. The specific extinction coefficient of benzoylformate at 340 nm was determined

in the same buffer as  $\epsilon = 0.032 \text{ L mmol}^{-1} \text{ cm}^{-1}$ . The reaction was examined at 30 °C for 90 s.

**Coupled decarboxylase assay:** The assay mixture was prepared from following stock solutions prepared in standard buffer: benzoylformate solution (100  $\mu\text{L}$ , 50 mM, adjusted to pH 6.0), NADH (100  $\mu\text{L}$ , 3.5 mM), HLADH (50  $\mu\text{L}$ , 10 U, Sigma) and potassium phosphate buffer (700  $\mu\text{L}$ , 50 mM, pH 6.0). The components were mixed in a 1.7 mL cuvette, incubated for 3 min at 30 °C, and the reaction was started by addition of BFD solution (50  $\mu\text{L}$ , 0.05 U). The descending curve was examined at 340 nm and the linear slope was calculated from 15–90 s.

**Decarboxylation of other 2-keto acids:** To detect low activities towards unnatural substrates in the coupled assay, the substrate and enzyme concentrations were increased to 20 mM and 0.5 U, respectively. Further, the reaction time was extended to 3 min. A control containing all assay components except BFD was performed in order to detect any non-catalytic decarboxylation effects.

**pH influence on the enzyme stability and activity:** *i) stability:* The stability of BFD towards pH modifications was investigated in 2 mL batches by adjusting the standard buffer to the desired pH value. After addition of BFD–His (50  $\mu\text{L}$ , 1 U), samples were taken in time intervals of 5–10 min and analyzed for residual activity using the coupled decarboxylase assay. *ii) decarboxylase activity:* The direct decarboxylase assay was performed at various pH values between 4.0 and 8.0 by adjusting the standard buffer solution to the desired pH values with  $\text{H}_3\text{PO}_4$  (0.1 M) or KOH (0.1 M). *iii) carboligase activity:* The pH optimum of the carboligation reaction was measured in 1.5 mL batches. Benzoylformate (100 mM),  $\text{MgSO}_4$  (2.5 mM), ThDP (0.15 mM), and acetaldehyde (500 mM) were dissolved in potassium phosphate buffer (1.5 mL, 200 mM), adjusted to the respective pH, and BFD–His (17 U) was added. The reaction was stopped after 3 h at 25 °C by heating the mixture to 95 °C. Subsequently, the amount of 2-HPP formed was determined by HPLC (RP-C18 column; see below).

**Temperature influence on enzyme stability and activity:** *i) stability:* The stability of BFD–His towards elevated temperatures was studied in 2 mL batches with BFD–His (1 U) in standard buffer at 25 °C, 40 °C, 60 °C, and 80 °C. In intervals of 5–10 min aliquots (50  $\mu\text{L}$ ) were taken and analyzed for residual activity using the coupled decarboxylase assay. *ii) decarboxylase activity:* The dependence of the decarboxylase activity on the reaction temperature was determined using the direct decarboxylase assay by stepwise increasing the assay temperature from 25 °C to 68 °C. *iii) carboligase activity:* The carboligation activity was measured using 1 mL batches containing benzaldehyde (50 mM) and acetaldehyde (500 mM) in standard buffer, pH 6.9. After addition of BFD–His (6.4 U) samples were incubated at various temperatures between 10 °C and 50 °C. The reactions were stopped at conversions between 5 and 10% (starting conditions) by heat inactivation of the enzyme. Benzaldehyde and 2-HPP were assayed by HPLC on a RP-C18 column (see below).

**Synthesis of 2-hydroxy ketones:** Analytical scale synthesis of the 2-hydroxy ketones given in Table 4 were carried out in 1.5 mL batches using potassium phosphate buffer (50 mM, pH 7.0), containing the acyl donor aldehyde (10 mM, or the maximum soluble amount), and acetaldehyde (500 mM) as an acceptor. Reactions were performed with wt-BFD (6.75 U) for 20 h at room temperature without shaking or stirring. Subsequently, the reaction mixture was extracted with *n*-heptane (0.3 mL) or trichloromethane followed by phase separation by centrifugation (13000 rpm). The organic layer was dried over  $\text{MgSO}_4$  and 2-hydroxy ketones were analyzed by GC-MS and chiral phase HPLC or GC. Synthesis and analysis of acetoin was performed as described elsewhere.<sup>[43]</sup>

**(S)-2-Hydroxy-1-(2-methylphenyl)-propanone (4b):** Conversion 4%; *ee* n.d.; GC-MS:  $t_{\text{R}} = 8.4$  min;  $m/z$  (%): 164 (0.8)  $[M]^+$ , 119 (100)  $[M - \text{C}_2\text{H}_5\text{O}]^+$ , 91 (38)  $[\text{C}_7\text{H}_7]^+$ , 65 (13)  $[\text{C}_3\text{H}_3]^+$ , 51 (2.4)  $[\text{C}_4\text{H}_3]^+$ .

**(S)-1-(2-Fluorophenyl)-2-hydroxy-propanone (4c):** Conv. 91%; *ee* 89%; HPLC (Chiralcel OB):  $t_{\text{R}}(S) = 10.8$  min,  $t_{\text{R}}(R) = 15.2$  min; GC-MS:  $t_{\text{R}} = 7.5$  min;  $m/z$  (%): 168 (0.5)  $[M]^+$ , 123 (100)  $[M - \text{C}_2\text{H}_5\text{O}]^+$ , 95 (47)  $[\text{C}_6\text{H}_4\text{F}]^+$ , 75 (16)  $[\text{C}_6\text{H}_3]^+$ , 51 (4.8)  $[\text{C}_4\text{H}_3]^+$ .

**(S)-1-(3-Fluorophenyl)-2-hydroxy-propanone (4d):** Conv. 100%; *ee* 87%; HPLC (Chiralcel OB):  $t_{\text{R}}(S) = 10.7$  min,  $t_{\text{R}}(R) = 14.6$  min; GC-MS:  $t_{\text{R}} = 7.5$  min;  $m/z$  (%): 168 (0.4)  $[M]^+$ , 123 (100)  $[M - \text{C}_2\text{H}_5\text{O}]^+$ , 95 (55)  $[\text{C}_6\text{H}_4\text{F}]^+$ , 75 (22)  $[\text{C}_6\text{H}_3]^+$ , 51 (4.1)  $[\text{C}_4\text{H}_3]^+$ .

**(S)-1-(3-Chlorophenyl)-2-hydroxy-propanone (4e):** Conv. 94%; *ee* 94%; HPLC (Chiralcel OB):  $t_{\text{R}}(S) = 10.9$  min,  $t_{\text{R}}(R) = 17.2$  min; GC-MS:

$t_{\text{R}} = 8.9$  min;  $m/z$  (%): 184 (1.5)  $[M]^+$ , 139 (100)  $[M - \text{C}_2\text{H}_5\text{O}]^+$ , 111 (44)  $[\text{C}_6\text{H}_4\text{Cl}]^+$ , 75 (26)  $[\text{C}_6\text{H}_3]^+$ , 50 (9.8)  $[\text{C}_4\text{H}_3]^+$ .

**(S)-1-(3-Bromophenyl)-2-hydroxy-propanone (4f):** Conv. 68%; *ee* 96%; HPLC (Chiralcel OB):  $t_{\text{R}}(S) = 12.5$  min,  $t_{\text{R}}(R) = 19.0$  min; GC-MS:  $t_{\text{R}} = 9.5$  min;  $m/z$  (%): 232 (1.6)  $[M]^+$ , 185 (100)  $[M - \text{C}_2\text{H}_5\text{O}]^+$ , 157 (40)  $[\text{C}_6\text{H}_4\text{Br}]^+$ , 75 (23)  $[\text{C}_6\text{H}_3]^+$ , 51 (8.1)  $[\text{C}_4\text{H}_3]^+$ .

**(S)-2-Hydroxy-1-(3-methylphenyl)-propanone (4g):** Conv. 99%; *ee* 97%; HPLC (Chiralcel OB):  $t_{\text{R}}(S) = 9.9$  min,  $t_{\text{R}}(R) = 19.3$  min; GC-MS:  $t_{\text{R}} = 8.1$  min;  $m/z$  (%): 164 (0.5)  $[M]^+$ , 119 (100)  $[M - \text{C}_2\text{H}_5\text{O}]^+$ , 91 (77)  $[\text{C}_7\text{H}_7]^+$ , 65 (29)  $[\text{C}_3\text{H}_3]^+$ , 51 (4.8)  $[\text{C}_4\text{H}_3]^+$ .

**(S)-2-Hydroxy-1-(3-methoxyphenyl)-propanone (4h):** Conv. 94%; *ee* 96%; HPLC (Chiralcel OB):  $t_{\text{R}}(S) = 17.8$  min,  $t_{\text{R}}(R) = 32.7$  min; GC-MS:  $t_{\text{R}} = 9.3$  min;  $m/z$  (%): 180 (26)  $[M]^+$ , 135 (100)  $[M - \text{C}_2\text{H}_5\text{O}]^+$ , 107 (59)  $[\text{C}_7\text{H}_7\text{O}]^+$ , 92 (31)  $[\text{C}_6\text{H}_4\text{O}]^+$ , 77 (45)  $[\text{C}_6\text{H}_3]^+$ , 64 (17)  $[\text{C}_3\text{H}_4]^+$ , 51 (4.8)  $[\text{C}_4\text{H}_3]^+$ .

**(S)-1-(3-Ethoxyphenyl)-2-hydroxy-propanone (4i):** Conv. 91%; *ee* 97%; HPLC (Chiralcel OB):  $t_{\text{R}}(S) = 14.6$  min,  $t_{\text{R}}(R) = 35.0$  min; GC-MS:  $t_{\text{R}} = 9.7$  min;  $m/z$  (%): 194 (25)  $[M]^+$ , 149 (100)  $[M - \text{C}_2\text{H}_5\text{O}]^+$ , 121 (60)  $[\text{C}_8\text{H}_9\text{O}]^+$ , 95 (19)  $[\text{C}_5\text{H}_5\text{O}_2]^+$ , 92 (12)  $[\text{C}_6\text{H}_4\text{O}]^+$ , 77 (23)  $[\text{C}_6\text{H}_3]^+$ , 65 (27)  $[\text{C}_3\text{H}_3]^+$ , 50 (3.2)  $[\text{C}_4\text{H}_2]^+$ .

**(S)-2-Hydroxy-1-(3-(isopropoxy)-phenyl)-propanone (4j):** Conv. 62%; *ee* > 99%; HPLC (Chiralcel OB):  $t_{\text{R}}(S) = 11.9$  min,  $t_{\text{R}}(R) = \text{n.d.}$ ; GC-MS:  $t_{\text{R}} = 9.9$  min;  $m/z$  (%): 208 (31)  $[M]^+$ , 163 (100)  $[M - \text{C}_2\text{H}_5\text{O}]^+$ , 121 (99)  $[\text{C}_8\text{H}_9\text{O}]^+$ , 93 (42)  $[\text{C}_6\text{H}_5\text{O}]^+$ , 77 (11)  $[\text{C}_6\text{H}_3]^+$ , 65 (26)  $[\text{C}_3\text{H}_3]^+$ , 50 (3.2)  $[\text{C}_4\text{H}_2]^+$ .

**(S)-2-Hydroxy-1-(3-methoxymethoxyphenyl)-propanone (4k):** Conv. 88%; *ee* > 99%; HPLC (Chiralcel OB, *iso*-hexane/isopropanol = 85:15, flow 0.75 mL min<sup>-1</sup>, 25 °C):  $t_{\text{R}}(S) = 25.7$  min,  $t_{\text{R}}(R) = \text{n.d.}$ ; GC-MS:  $t_{\text{R}} = 10.1$  min;  $m/z$  (%): 210 (7.6)  $[M]^+$ , 165 (100)  $[M - \text{C}_2\text{H}_5\text{O}]^+$ , 135 (22)  $[M - \text{C}_3\text{H}_5\text{O}_2]^+$ , 121 (15)  $[\text{C}_7\text{H}_5\text{O}_2]^+$ , 107 (10)  $[\text{C}_7\text{H}_7\text{O}]^+$ , 93 (3.5)  $[\text{C}_6\text{H}_5\text{O}]^+$ , 77 (9.5)  $[\text{C}_6\text{H}_3]^+$ , 65 (3.4)  $[\text{C}_3\text{H}_3]^+$ , 50 (2.3)  $[\text{C}_4\text{H}_2]^+$ .

**(S)-1-(3-Acetoxyphenyl)-2-hydroxy-propanone (4l):** Conv. 80%; *ee* > 99%; HPLC (Chiralcel OB):  $t_{\text{R}}(S) = 38.1$  min,  $t_{\text{R}}(R) = \text{n.d.}$ ; GC-MS:  $t_{\text{R}} = 10.1$  min;  $m/z$  (%): 208 (1.2)  $[M]^+$ , 165 (34)  $[M - \text{C}_2\text{H}_5\text{O}]^+$ , 163 (44)  $[M - \text{C}_2\text{H}_5\text{O}]^+$ , 121 (100)  $[\text{C}_8\text{H}_9\text{O}]^+$ , 95 (23)  $[\text{C}_3\text{H}_3\text{O}_2]^+$ , 93 (21)  $[\text{C}_6\text{H}_5\text{O}]^+$ , 77 (8.1)  $[\text{C}_6\text{H}_3]^+$ , 65 (13)  $[\text{C}_3\text{H}_3]^+$ , 50 (1.6)  $[\text{C}_4\text{H}_2]^+$ .

**(S)-2-Hydroxy-1-(3-hydroxyphenyl)-propanone (4m):** Conv. 62%; *ee* 92%; HPLC (Chiralcel OB):  $t_{\text{R}}(S) = 12.9$  min,  $t_{\text{R}}(R) = 14.4$  min; GC-MS:  $t_{\text{R}} = 10.0$  min;  $m/z$  (%): 166 (9.7)  $[M]^+$ , 121 (100)  $[M - \text{C}_2\text{H}_5\text{O}]^+$ , 95 (42)  $[\text{C}_3\text{H}_3\text{O}_2]^+$ , 93 (35)  $[\text{C}_6\text{H}_5\text{O}]^+$ , 77 (25)  $[\text{C}_6\text{H}_3]^+$ , 65 (26)  $[\text{C}_3\text{H}_3]^+$ , 51 (4.0)  $[\text{C}_4\text{H}_3]^+$ .

**(S)-1-(3-Cyanophenyl)-2-hydroxy-propanone (4n):** Conv. 95%; *ee* 92%; HPLC (Chiralcel OB):  $t_{\text{R}}(S) = 39.8$  min,  $t_{\text{R}}(R) = 56.59$  min; GC-MS:  $t_{\text{R}} = 9.8$  min;  $m/z$  (%): 175 (1.9)  $[M]^+$ , 147 (39)  $[M - \text{CO}]^+$ , 130 (87)  $[M - \text{C}_2\text{H}_5\text{O}]^+$ , 103 (100)  $[\text{C}_7\text{H}_5\text{N}]^+$ , 76 (22)  $[\text{C}_6\text{H}_4]^+$ , 51 (11)  $[\text{C}_4\text{H}_3]^+$ .

**(S)-1-(4-Fluorophenyl)-2-hydroxy-propanone (4o):** Conv. 69%; *ee* 87%; HPLC (Chiralcel OB):  $t_{\text{R}}(S) = 11.6$  min,  $t_{\text{R}}(R) = 18.1$  min; GC-MS:  $t_{\text{R}} = 7.6$  min;  $m/z$  (%): 168 (0.4)  $[M]^+$ , 123 (100)  $[M - \text{C}_2\text{H}_5\text{O}]^+$ , 95 (31)  $[\text{C}_6\text{H}_4\text{F}]^+$ , 75 (9.7)  $[\text{C}_6\text{H}_3]^+$ , 51 (1.6)  $[\text{C}_4\text{H}_3]^+$ .

**(S)-1-(4-Chlorophenyl)-2-hydroxy-propanone (4p):** Conv. 85%; *ee* 82%; HPLC (Chiralcel OB):  $t_{\text{R}}(S) = 10.9$  min,  $t_{\text{R}}(R) = 14.7$  min; GC-MS:  $t_{\text{R}} = 8.9$  min;  $m/z$  (%): 184 (1.0)  $[M]^+$ , 139 (100)  $[M - \text{C}_2\text{H}_5\text{O}]^+$ , 111 (27)  $[\text{C}_6\text{H}_4\text{Cl}]^+$ , 75 (14)  $[\text{C}_6\text{H}_3]^+$ , 51 (3.5)  $[\text{C}_4\text{H}_3]^+$ .

**(S)-1-(4-Bromophenyl)-2-hydroxy-propanone (4q):** Conv. 42%; *ee* 83%; HPLC (Chiralcel OB):  $t_{\text{R}}(S) = 11.5$  min,  $t_{\text{R}}(R) = 14.4$  min; GC-MS:  $t_{\text{R}} = 9.6$  min;  $m/z$  (%): 232 (0.4)  $[M]^+$ , 185 (100)  $[M - \text{C}_2\text{H}_5\text{O}]^+$ , 157 (38)  $[\text{C}_6\text{H}_4\text{Br}]^+$ , 75 (22)  $[\text{C}_6\text{H}_3]^+$ , 50 (15)  $[\text{C}_4\text{H}_2]^+$ .

**(S)-2-Hydroxy-1-(4-methylphenyl)-propanone (4r):** Conv. 65%; *ee* 88%; HPLC (Chiralcel OB):  $t_{\text{R}}(S) = 10.8$  min,  $t_{\text{R}}(R) = 19.6$  min; GC-MS:  $t_{\text{R}} = 8.6$  min;  $m/z$  (%): 164 (0.4)  $[M]^+$ , 119 (100)  $[M - \text{C}_2\text{H}_5\text{O}]^+$ , 91 (77)  $[\text{C}_7\text{H}_7]^+$ , 65 (32)  $[\text{C}_3\text{H}_3]^+$ , 51 (4.8)  $[\text{C}_4\text{H}_3]^+$ .

**(S)-2-Hydroxy-1-(4-methoxyphenyl)-propanone (4s):** Conv. 23%; *ee* 92%; HPLC (Chiralcel OB):  $t_{\text{R}}(S) = 20.2$  min,  $t_{\text{R}}(R) = 30.2$  min; GC-MS:  $t_{\text{R}} = 9.7$  min;  $m/z$  (%): 180 (7.3)  $[M]^+$ , 135 (100)  $[M - \text{C}_2\text{H}_5\text{O}]^+$ , 107 (19)  $[\text{C}_7\text{H}_7\text{O}]^+$ , 92 (21)  $[\text{C}_6\text{H}_4\text{O}]^+$ , 77 (30)  $[\text{C}_6\text{H}_3]^+$ , 64 (10)  $[\text{C}_3\text{H}_4]^+$ , 51 (4.8)  $[\text{C}_4\text{H}_3]^+$ .

**(S)-2-Hydroxy-1-(4-hydroxyphenyl)-propanone (4t):** Conv. 11%; *ee* 86%; HPLC (Chiralcel OB):  $t_{\text{R}}(S) = 15.6$  min,  $t_{\text{R}}(R) = 21.2$  min; GC-MS:

$t_R = 10.3$  min;  $m/z$  (%): 166 (3.1)  $[M]^+$ , 121 (100)  $[M - C_2H_5O]^+$ , 93 (16)  $[C_6H_5O]^+$ , 77 (5.0)  $[C_6H_5]^+$ , 65 (13)  $[C_5H_5]^+$ , 51 (1.5)  $[C_4H_5]^+$ .

**(S)-1-(4-Cyanophenyl)-2-hydroxy-propanone (4u):** Conv. 89%;  $ee$  74%; HPLC (Chiralcel OB):  $t_R(S) = 37.9$  min,  $t_R(R) = 52.4$  min; GC-MS:  $t_R = 9.7$  min;  $m/z$  (%): 175 (0.2)  $[M]^+$ , 130 (100)  $[M - C_2H_5O]^+$ , 103 (74)  $[C_7H_5N]^+$ , 76 (22)  $[C_6H_4]^+$ , 51 (14)  $[C_4H_5]^+$ .

**(S)-1-(3,5-Difluorophenyl)-2-hydroxy-propanone (4v):** Conv. 93%;  $ee$  81%; HPLC (Chiralcel OB):  $t_R(S) = 8.7$  min,  $t_R(R) = 10.5$  min; GC-MS:  $t_R = 7.1$  min;  $m/z$  (%): 186 (1.8)  $[M]^+$ , 141 (100)  $[M - C_2H_5O]^+$ , 113 (70)  $[C_6H_3F_2]^+$ , 95 (11)  $[C_6H_4F]^+$ , 63 (29)  $[C_5H_3]^+$ , 51 (1.1)  $[C_4H_3]^+$ .

**(S)-2-Hydroxy-1-(3,5-dimethoxyphenyl)-propanone (4w):** Conv. 11%;  $ee > 99\%$ ; HPLC (Chiralcel OB):  $t_R(S) = 21.1$  min,  $t_R(R) = n.d.$ ; GC-MS:  $t_R = 10.6$  min;  $m/z$  (%): 210 (27)  $[M]^+$ , 165 (100)  $[M - C_2H_5O]^+$ , 137 (30)  $[M - C_3H_5O_2]^+$ , 122 (23)  $[C_7H_6O_2]^+$ , 107 (13)  $[C_6H_5O_2]^+$ , 77 (10)  $[C_6H_5]^+$ , 63 (6.4)  $[C_5H_5]^+$ , 51 (3.4)  $[C_4H_5]^+$ .

**(S)-1-(Furan-2-yl)-2-hydroxy-propanone (7a):** Conv. 56%;  $ee$  45%; HPLC (Chiralcel OB):  $t_R(S) = 19.7$  min,  $t_R(R) = 27.1$  min; GC-MS:  $t_R = 6.4$  min;  $m/z$  (%): 140 (3.7)  $[M]^+$ , 95 (100)  $[M - C_2H_5O]^+$ , 68 (15)  $[C_4H_4O]^+$ , 51 (1.6)  $[C_4H_3]^+$ .

**(S)-2-Hydroxy-1-(thiophene-2-yl)-propanone (7b):** Conv. 50%;  $ee$  83%; HPLC (Chiralcel OB):  $t_R(S) = 23.1$  min,  $t_R(R) = 30.7$  min; GC-MS:  $t_R = 7.9$  min;  $m/z$  (%): 156 (1.9)  $[M]^+$ , 111 (100)  $[M - C_2H_5O]^+$ , 83 (9.8)  $[C_4H_5S]^+$ , 50 (1.5)  $[C_4H_5]^+$ .

**(S)-2-Hydroxy-1-(pyridine-3-yl)-propanone (8):** Conv. 65%;  $ee$  87%; HPLC (Chiralcel OB):  $t_R(S) = 20.1$  min,  $t_R(R) = 23.0$  min; GC-MS:  $t_R = 8.0$  min;  $m/z$  (%): 151 (0.7)  $[M]^+$ , 106 (97)  $[M - C_2H_5O]^+$ , 79 (100)  $[C_5H_5N]^+$ , 51 (38)  $[C_4H_5]^+$ .

**(S)-1-Cyclohexyl-2-hydroxy-propanone (9):** Conv. 21%;  $ee$  61%; GC (Cyclodex  $\beta$ -I/P):  $t_R(S) = 17.1$  min,  $t_R(R) = 17.9$  min; GC-MS:  $t_R = 7.4$  min;  $m/z$  (%): 156 (0.6)  $[M]^+$ , 111 (33)  $[M - C_2H_5O]^+$ , 95 (21)  $[C_5H_5O_2]^+$ , 83 (100)  $[C_6H_{11}]^+$ , 55 (42)  $[C_4H_7]^+$ .

**(S)-1-(Cyclohex-1-enyl)-2-hydroxy-propanone (10):** Conv. 50%;  $ee$  94%; HPLC (Chiralcel OB):  $t_R(S) = 11.0$  min,  $t_R(R) = 19.9$  min; GC-MS:  $t_R = 8.0$  min;  $m/z$  (%): 154 (7.3)  $[M]^+$ , 109 (100)  $[M - C_2H_5O]^+$ , 81 (62)  $[C_6H_9]^+$ , 53 (11)  $[C_4H_5]^+$ .

**(S)-2-Hydroxy-1-phenyl-propanone (4a):** A typical experiment was performed in a 50 mL batch with benzaldehyde (50 mm) or benzoylformate (100 mm) and acetaldehyde (500 mm) in standard buffer. Depending on the substrate, the pH value was adjusted to 6.5 (benzoylformate) or 7.0 (benzaldehyde). In the case of benzoylformate pH control was required. The reaction was started by addition of BFD (50 U) and subsequently stopped after adequate conversion by extracting the crude product as described above. The solvent was removed in vacuo, and the crude product purified by column chromatography (SiO<sub>2</sub>, diethyl ether/*n*-hexane 3:1 *v/v*,  $R_f = 0.49$ ). Using benzaldehyde as substrate the reaction was stopped after 5 h (150 mg, 40% yield,  $ee$  90%). The reaction using benzoylformate was stopped after 18 h (74 mg, 10% yield,  $ee$  92%). Under optimized reaction conditions the  $ee$  increased to 95%.  $[\alpha]_D^{25} = -79.2$  ( $c = 0.016$  in trichloromethane). <sup>1</sup>H NMR (300 MHz, CDCl<sub>3</sub>, 20 °C):  $\delta = 1.47$  (d, 3H, <sup>3</sup>*J*(H,H) = 7.0 Hz; CH<sub>3</sub>), 3.81 (br, 1H; OH), 5.19 (q, 1H, <sup>3</sup>*J*(H,H) = 7.0 Hz; CHOH), 7.52 ("t", 2H, <sup>3</sup>*J*(H,H) = 7.5 Hz; Ar-H), 7.64 (tt, 1H, <sup>3</sup>*J*(H,H) = 7.5 Hz, <sup>4</sup>*J*(H,H) = 1.3 Hz; Ar-H), 7.95 (dd, 2H, <sup>3</sup>*J*(H,H) = 7.5 Hz, <sup>4</sup>*J*(H,H) = 1.3 Hz; Ar-H); <sup>13</sup>C NMR (75.5 MHz, CDCl<sub>3</sub>, 20 °C):  $\delta = 22.74$  (CH<sub>3</sub>), 69.73 (CHOH), 129.09, 129.31 (CH), 133.71 (C<sub>q</sub>), 134.44 (CH), 202.82 (CO); GC-MS:  $t_R = 7.7$  min;  $m/z$  (%): 150 (0.2)  $[M]^+$ , 135 (1.3)  $[M - CH_3]^+$ , 105 (100)  $[C_7H_7O]^+$ , 77 (57)  $[C_6H_5]^+$ , 51 (17)  $[C_5H_5]^+$ ; HPLC (RP-C18):  $t_R = 12.2$  min (2-HPP);  $t_R = 18.3$  min (benzaldehyde); HPLC (Chiralcel OB):  $t_R(S) = 13.4$  min;  $t_R(R) = 21.4$  min;<sup>[44]</sup> GC (Cyclodex  $\beta$ -I/P):  $t_R(S) = 22.1$  min;  $t_R(R) = 22.7$  min.

**(R)-Benzoin (5):** A typical fed-batch reaction was performed in a 100 mL batch equipped with a magnetic stirrer. Benzaldehyde (50 mm) was dissolved in potassium phosphate buffer (100 mL, 50 mM, pH 7.0), containing MgSO<sub>4</sub> (2.5 mM) and ThDP (0.15 mM). After addition of BFD (150 U) the reaction was stirred slowly for 7 h at room temperature. (*R*)-Benzoin was extracted as described above. The crude product was dissolved in diethyl ether/*n*-hexane (1:1 *v/v*) and pure (*R*)-benzoin precipitated at -20 °C with *n*-hexane. The product was collected by filtration, washed with ice-cold *n*-hexane and dried in vacuo. Optical purity was examined by <sup>1</sup>H NMR using tris[3-(trifluoromethyl-hydroxy-methylene-(+)-camphora-

to]-europium as a shift reagent and by chiral phase HPLC. With both methods only the (*R*)-enantiomer was detectable which is in accord with the optical purity determined in the crude product (4.3 mg, 0.4% yield). M.p.: 133 °C;  $ee > 99\%$ ;  $[\alpha]_D^{25} = 109.8$  ( $c = 0.007$  in acetone); <sup>1</sup>H NMR (300 MHz, CDCl<sub>3</sub>, 20 °C, TMS):  $\delta = 4.56$  (br, 1H; OH), 5.95 (s, 1H; CHOH), 7.5 (m, 6H; Ar-H), 7.9 (m, 4H; Ar-H); GC-MS:  $t_R = 11.3$  min;  $m/z$  (%): 212 (0.5)  $[M]^+$ , 105 (100)  $[C_7H_7O]^+$ , 77 (40)  $[C_6H_5]^+$ , 51 (9.8)  $[C_4H_5]^+$ ; HPLC (Chiralcel OB, isohexane/isopropanol 95:5, flow 0.75 mL min<sup>-1</sup>, 20 °C):  $t_R(S) = 37.4$  min;  $t_R(R) = 50.3$  min (only the (*R*)-enantiomer was detected in the enzymatic preparation<sup>[45]</sup>).

**Continuous synthesis of (S)-2-HPP (4a) in the enzyme membrane reactor:** The substrate solution (10 mM benzaldehyde, 100 mM acetaldehyde, 4 mM ThDP, 0.5 mM MgCl<sub>2</sub>, 50 mM potassium phosphate buffer pH 7) was pumped through a continuously operated stirred tank reactor (reactor volume 10 mL) containing a hydrophilic ultrafiltration membrane (Diaflo YM20, cut off 20000 Da, Amicon, Frankfurt, Germany). Prior to use, the membrane was equilibrated with water. To prevent adsorption of the BFD on the membrane, the membrane was pre-coated with 50 mg bovine serum albumin. Since benzaldehyde is absorbed by the reactor material polypropylene, the reactor was flushed with substrate solution until influx and efflux showed the same benzaldehyde concentration. The reaction was started by injecting 300 U BFD. The residence time was controlled by the flow of the substrate solution. The resulting product was isolated using standard methods (see above). Space-time yield: 34.2 g L<sup>-1</sup> d<sup>-1</sup> (220 mmol L<sup>-1</sup> d<sup>-1</sup>); conv. 90%;  $ee$  92.5%.

## Acknowledgement

This work has been supported by the Deutsche Forschungsgemeinschaft in the scope of SFB 380. We are grateful to Prof. Dr. G. Kenyon (UCSF, USA) for providing the vector pBFD/trc, and to Dr. M. Hasson (Purdue University, USA) for providing structural data of BFD prior to the data base release. A.S.D. thanks for Alexander von Humboldt Fellowship.

- [1] G. D. Hegeman, *Methods Enzymol.* **1970**, *17*, 674–678.
- [2] M. M. Barrowman, W. Harnett, A. J. Scott, C. A. Fewson, J. R. Kusel, *FEMS Microbiol. Lett.* **1986**, *34*, 57–60.
- [3] M. M. Barrowman, C. A. Fewson, *Curr. Microbiol.* **1985**, *12*, 235–240.
- [4] A. Y. Tsou, S. C. Ransom, J. A. Gerlt, D. D. Buechter, P. C. Babbitt, G. L. Kenyon, *Biochemistry* **1990**, *29*, 9856–9862.
- [5] M. S. Hasson, A. Muscate, M. J. McLeish, L. S. Polovnikova, J. A. Gerlt, G. L. Kenyon, G. A. Petsko, D. Ringe, *Biochemistry* **1998**, *37*, 9918–9930.
- [6] Y. A. Muller, G. E. Schulz, *Science* **1993**, *25*, 965–967.
- [7] D. Dobritzsch, S. König, G. Schneider, G. G. Lu, *J. Biol. Chem.* **1998**, *273*, 20196–20204.
- [8] P. M. Weiss, G. A. Garcia, G. L. Kenyon, W. W. Cleland, P. F. Cook, *Biochemistry* **1988**, *27*, 2197–2205.
- [9] L. J. Reynolds, G. A. Garcia, J. W. Kozarich, G. L. Kenyon, *Biochemistry* **1988**, *27*, 5530–5538.
- [10] A. Schellenberger, *Biochim. Biophys. Acta* **1998**, *1385*, 177–186.
- [11] For recent reviews of ThDP-dependent enzymes see: a) G. A. Sprenger, M. Pohl, *J. Mol. Catal. B: Enzym.* **1999**, *6*, 145–159; b) U. Schörken, G. A. Sprenger, *Biochim. Biophys. Acta* **1998**, *1385*, 229–243.
- [12] M. Pohl, *Adv. Biochem. Eng. Biotechnol.* **1997**, *58*, 16–43.
- [13] H. Iding, P. Siebert, K. Mesch, M. Pohl, *Biochim. Biophys. Acta* **1998**, *1385*, 307–322.
- [14] W.-D. Fessner, C. Walter, *Top. Curr. Chem.* **1996**, *184*, 97–194.
- [15] R. A. Sheldon, *Chirotechnology: Industrial Synthesis of Optically Active Compounds*, Marcel Dekker, New York, **1993**.
- [16] a) R. Kluger, J. F. Lam, J. P. Pezacki, C.-M. Yang, *J. Am. Chem. Soc.* **1995**, *117*, 11383–11389; b) R. Kluger, *Pure Appl. Chem.* **1997**, *69*, 1957–1967.
- [17] D. Kern, G. Kern, H. Neef, K. Tittmann, M. Killenberg-Jabs, C. Wikner, G. Schneider, G. Hübner, *Science* **1997**, *275*, 67–70.
- [18] J. P. Kuebrich, R. L. Schowen, M. Wang, M. E. Lupes, *J. Am. Chem. Soc.* **1971**, *93*, 1214–1223.

- [19] a) T. Ukai, R. Tanaka, T. Dokawa, *J. Pharm. Soc. Jpn.* **1943**, *63*, 296–300; b) H. Stetter, Y. Rämisch, H. Kuhlmann, *Synthesis* **1976**, 733–735; c) T. Matsumoto, M. Ohishi, S. Inoue, *J. Org. Chem.* **1985**, *50*, 603–606; d) J. Castells, F. López-Calahorra, L. Domingo, *J. Org. Chem.* **1988**, *53*, 4433–4436.
- [20] a) D. Enders, K. Breuer, *Helv. Chim. Acta* **1996**, *79*, 1217–1221; b) R. L. Knight, F. J. Leeper, *J. Chem. Soc. Perkin Trans. 1* **1998**, 1891–1893.
- [21] a) S. Hanessian, *Total Synthesis of Natural Products: The Chiron Approach*, Pergamon, New York, **1983**, Ch. 2; b) J. Polonský, *Fortis. Chem. Org. Naturst.* **1985**, *47*, 221–264; c) A. G. Chaudhary, D. G. I. Kingston, *Tetrahedron Lett.* **1993**, *34*, 4921–4924; d) D. Gala, D. J. DiBenedetto, J. E. Clark, B. L. Murphy, D. P. Schumacher, M. Steinman, *Tetrahedron Lett.* **1996**, *37*, 611–614; e) G. M. Coppola, H. F. Schuster,  *$\alpha$ -Hydroxy Acids in Enantioselective Synthesis*, VCH, Weinheim, **1997**.
- [22] W. Adam, M. Müller, F. Prechtel, *J. Org. Chem.* **1994**, *59*, 2358–2364.
- [23] W. Adam, R. T. Fell, V. R. Stegmann, C. H. Saha-Möller, *J. Am. Chem. Soc.* **1998**, *120*, 708–714.
- [24] W. Adam, R. T. Fell, C. R. Saha-Möller, C.-G. Zhao, *Tetrahedron: Asymmetry* **1998**, *9*, 397–401.
- [25] a) F. A. Davies, B.-C. Chen, *Chem. Rev.* **1992**, *92*, 919–934; b) T. Hashiyama, K. Morikawa, K. B. Sharpless, *J. Org. Chem.* **1992**, *57*, 5067–5068.
- [26] a) R. Csuk, B. I. Glänzer, *Chem. Rev.* **1991**, *91*, 49–97; b) K. Nakamura, S. Kondo, Y. Kawai, K. Hida, K. Kitano, A. Ohno, *Tetrahedron: Asymmetry* **1996**, *7*, 409–412.
- [27] W. Adam, R. T. Fell, U. Hoch, C. R. Saha-Möller, P. Schreiber, *Tetrahedron: Asymmetry* **1995**, *6*, 1047–1050.
- [28] W. Adam, M. T. Díaz, R. T. Fell, C. R. Saha-Möller, *Tetrahedron: Asymmetry* **1996**, *7*, 2207–2210.
- [29] a) C. Tanyeli, A. S. Demir, E. Dikici, *Tetrahedron: Asymmetry* **1996**, *7*, 2399–2402; b) A. S. Demir, H. Hamamci, C. Tanyeli, I. M. Akhmedov, F. Doganel, *Tetrahedron: Asymmetry* **1998**, *9*, 1673–1677.
- [30] a) C. Neuberg, J. Hirsch, *Biochem. Z.* **1921**, *115*, 282–310; b) C. Neuberg, H. Ohle, *Biochem. Z.* **1922**, *128*, 610–618; c) G. Hildebrandt, W. Klavehn, US 1956950, **1934** [*Chem. Abstr.* **1934**, 28, 40723]; d) H. Pfanz, D. Heise, Ger. (East) 13683, **1957** [*Chem. Abstr.* **1959**, 53, 8533d].
- [31] R. Wilcocks, O. P. Ward, S. Collins, N. J. Dewdney, Y. Hong, E. Prosen, *Appl. Environ. Microbiol.* **1992**, *58*, 1699–1704.
- [32] R. Wilcocks, O. P. Ward, *Biotechnol. Bioeng.* **1992**, *39*, 1058–1063.
- [33] M. S. Hasson, A. Muscate, G. T. M. Henehan, P. F. Guidinger, G. A. Petsko, D. Ringe, G. L. Kenyon, *Protein Sci.* **1995**, *4*, 955–959.
- [34] R. J. Diefenbach, R. G. Duggleby, *Biochem. J.* **1991**, *276*, 439–445.
- [35] a) R. Wichmann, C. Wandrey, A. F. Bückmann, M.-R. Kula, *Biotechnol. Bioeng.* **1981**, *23*, 2789–2802; b) U. Kragl, D. Vasic-Racki, C. Wandrey, *Chem. Ing.-Tech.* **1992**, *64*, 499–509; c) A. Liese, T. Zelinski, M.-R. Kula, H. Kierkels, M. Karutz, U. Kragl, C. Wandrey, *J. Mol. Cat. B: Enzym.* **1998**, *4*, 91–99.
- [36] Inspection of the active site of BFD was performed by computer modeling using the programs WHATIF and GRASP; see: G. Vriend, *J. Mol. Graph.* **1990**, *8*, 52–56.
- [37] S. K. Burley, G. A. Petsko, *Science* **1985**, *229*, 23–28.
- [38] a) O. Levenspiel, *Chemical Reaction Engineering*, 2nd ed., Wiley, New York, **1998**; b) U. Kragl, A. Liese in *The Encyclopedia of Bioprocess Technology: Fermentation, Biocatalysis and Bioseparation* (Eds.: M. C. Flickinger, S. W. Drew), Wiley, New York, **1999**, pp. 454–464; c) M. Biselli, U. Kragl, C. Wandrey in *Enzyme Catalysis in Organic Synthesis* (Eds.: K. Drauz, H. Waldmann), VCH, Weinheim, **1993**, pp. 89–155.
- [39] P. C. Traas, H. Boelens, H. J. Takken, *Tetrahedron Lett.* **1976**, *26*, 2287–2288.
- [40] D. S. Morris, *J. Chem. Soc.* **1950**, 1913–1917.
- [41] Y. Honda, A. Ori, G. Tsuchihashi, *Bull. Chem. Soc. Jpn.* **1987**, *60*, 1027–1036.
- [42] S. Hartmans, J. P. Smits, M. J. van der Werf, F. Volkerling, J. A. M. De Bont, *Appl. Environ. Microbiol.* **1989**, *55*, 2850.
- [43] M. Pohl, P. Siegert, K. Mesch, H. Bruhn, J. Grötzinger, *Eur. J. Biochem.* **1998**, *257*, 538–546.
- [44] *rac*-2-HPP was synthesized as standard for the enantiomer separation by HPLC according to J. P. McCormick, W. Tomasik, M. W. Johnson, *Tetrahedron Lett.* **1981**, *32*, 607–610.
- [45] Commercially available *rac*-benzoin (Aldrich) was used as standard for the enantiomer separation by HPLC.

Received: July 19, 1999 [F1927]